

This is the author's final, peer-reviewed manuscript as accepted for publication (AAM). The version presented here may differ from the published version, or version of record, available through the publisher's website. This version does not track changes, errata, or withdrawals on the publisher's site.

# Vibrational and conformational study of 1,3-Diaminopropane and its N-Deuterated and N-Ionised derivatives

S.R.O. Mendes, A.M. Amado, J. Tomkinson,  
M.P.M. Marques, and L.A.E. Batista de Carvalho

## Published version information

**Citation:** SRO Mendes et al. "Vibrational and conformational study of 1,3-Diaminopropane and its N-Deuterated and N-Ionised derivatives." *New Journal of Chemistry*, vol. 41, no. 18 (2017): 10132-10147

**doi:** [10.1039/C7NJ00810D](https://doi.org/10.1039/C7NJ00810D)

This version is made available in accordance with publisher policies. Please cite only the published version using the reference above.

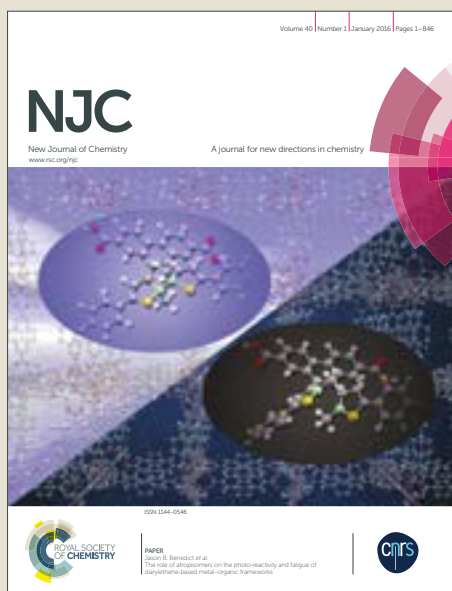
This item was retrieved from **ePubs**, the Open Access archive of the Science and Technology Facilities Council, UK. Please contact [epubs@stfc.ac.uk](mailto:epubs@stfc.ac.uk) or go to <http://epubs.stfc.ac.uk/> for further information and policies.

# NJC

Accepted Manuscript



This article can be cited before page numbers have been issued, to do this please use: S. R. O. Mendes, A. M. Amado, J. Tomkinson, M. P. M. Marques and L. A. E. Batista de Carvalho, *New J. Chem.*, 2017, DOI: 10.1039/C7NJ00810D.



This is an Accepted Manuscript, which has been through the Royal Society of Chemistry peer review process and has been accepted for publication.

Accepted Manuscripts are published online shortly after acceptance, before technical editing, formatting and proof reading. Using this free service, authors can make their results available to the community, in citable form, before we publish the edited article. We will replace this Accepted Manuscript with the edited and formatted Advance Article as soon as it is available.

You can find more information about Accepted Manuscripts in the [author guidelines](#).

Please note that technical editing may introduce minor changes to the text and/or graphics, which may alter content. The journal's standard [Terms & Conditions](#) and the ethical guidelines, outlined in our [author and reviewer resource centre](#), still apply. In no event shall the Royal Society of Chemistry be held responsible for any errors or omissions in this Accepted Manuscript or any consequences arising from the use of any information it contains.

## Vibrational and Conformational Study of 1,3-Diaminopropane and its N-Deuterated and N-Ionised Derivatives

S.R.O. Mendes,<sup>a</sup> A.M. Amado,<sup>a</sup> J. Tomkinson,<sup>b</sup> M.P.M. Marques,<sup>a,c</sup> and L.A.E. Batista de Carvalho<sup>a†</sup>

Received 00th January 20xx,  
Accepted 00th January 20xx

DOI: 10.1039/x0xx00000x

www.rsc.org/

A vibrational and conformational analysis of the linear alkylpolyamine 1,3-diaminopropane (1,3-dap) is reported, using vibrational spectroscopy (Raman, Fourier Transform Infrared (FTIR) and inelastic neutron scattering (INS)) coupled to theoretical approaches at the Density Functional Theory (DFT) level. The quantum mechanical calculations were carried out using the mPW1PW functional and the 6-31G\* basis set, for the isolated molecule, the condensed phase, and solutions in both water and carbon tetrachloride. The most stable geometries were calculated to be GGG'G and TG'GG' for the gaseous phase and the CCl<sub>4</sub> solution, and TTTT, TGTT and TTTG for the condensed phase and the aqueous solution. Since the relative populations obtained for the different 1,3-dap conformers were very similar, the corresponding experimental spectra reflect the presence of a mixture of species. The vibrational data obtained for 1,3-dap in its pure form – unprotonated, totally protonated (N-ionised) and N-deuterated – as well as for its aqueous and CCl<sub>4</sub> solutions, were assigned in the light of the theoretical results presently obtained and experimental data previously gathered for similar compounds.

### Introduction

Rotational isomerism in linear alkylamines, that has been the object of various studies,<sup>1-17</sup> is influenced by different factors, from steric and dipolar effects to hyperconjugative and hydrogen bonding interactions.<sup>5,9,11,14</sup> Moreover, the stability of this kind of systems is strongly dependent on the balance between intra and intermolecular interactions.<sup>8-10,16-18</sup>

Although polyamine crystals were found in human seminal liquid by Leeuwenhoek about three hundred years ago, only very recently has the biological importance of these compounds been acknowledged. In fact, both 1,3-diaminopropane (1,3-dap, H<sub>2</sub>N(CH<sub>2</sub>)<sub>3</sub>NH<sub>2</sub>) and 1,4-diaminobutane (1,4-dab, H<sub>2</sub>N(CH<sub>2</sub>)<sub>4</sub>NH<sub>2</sub>, putrescine), are precursors of the biogenic tri- and tetramines spermidine (spd, H<sub>2</sub>N(CH<sub>2</sub>)<sub>3</sub>NH(CH<sub>2</sub>)<sub>4</sub>NH<sub>2</sub>) and spermine (spm, H<sub>2</sub>N(CH<sub>2</sub>)<sub>3</sub>NH(CH<sub>2</sub>)<sub>4</sub>NH(CH<sub>2</sub>)<sub>3</sub>NH<sub>2</sub>), that play key physiological functions, namely in eukaryotic cell proliferation and differentiation. Since changes in their biological levels are known to be responsible for a significant effect on cellular proliferation and DNA replication, intracellular polyamine levels are related to carcinogenesis and neoplastic growth.<sup>19</sup> Up to this date, several studies have reported different biological functions for 1,3-dap, namely: regulator of ornithine decarboxylase (ODC, one of the main enzymes involved in the polyamine biosynthetic pathway)<sup>20,21</sup> and carcinogen biomarker.<sup>22,23</sup> However, the exact nature of the mechanisms involved, at a molecular level, is still unknown, which highlights

the relevance of gathering detailed structural and conformational information on this compound, in order to understand its main biochemical role. Actually, few structural and spectroscopic studies have been performed for this system and even these are limited to narrow regions of the vibrational spectra.<sup>18,24,25</sup> 1,3-dap is also quite relevant at an industrial level, namely in food and pharmaceutical industries. Regarding the latter, it may be used for the design of new diuretic<sup>26</sup> and anticancer<sup>27-30</sup> drugs.

Cancer is one of the pathologies with the greatest impact on society, responsible for a high annual mortality rate.<sup>31</sup> Currently, cisplatin (cis-diaminedichloroplatin (II)) is one of the most widely used and effective chemotherapeutic agent.<sup>32-33</sup> However, it acts in a narrow range of tumours and is associated to severe side effects such as neurotoxicity,<sup>34</sup> ototoxicity<sup>35</sup> and nephrotoxicity,<sup>36</sup> as well as to acquired resistance that limits its prolonged clinical administration. To overcome these limitations and mitigate the deleterious side effects of chemotherapy is a challenging goal that may be achieved through the rational design of new anticancer agents, namely polynuclear platinum and palladium complexes with linear polyamines (biogenic polyamines and their analogues). In fact, this type of Pt(II) and Pd(II)-polyamine chelates was shown to display promising cytotoxic properties *via* an unconventional interaction with DNA.<sup>27-30,33,37-44</sup>

With a view to understand both the antitumor activity of these compounds and the structural dependence of such activity, it is crucial to have a deep knowledge of their aliphatic ligands. Hence, the present work aimed at a conformational study of 1,3-dap, one of the smallest diamines, as well as its N-ionised derivative, using DFT methods and vibrational spectroscopy (both optical – Raman and FTIR – and neutron scattering techniques). The changes in the corresponding conformational

<sup>a</sup> Unidade de I&D “Química-Física Molecular”, Department of Chemistry, University of Coimbra, 3004-535 Coimbra, Portugal

<sup>b</sup> ISIS Facility, STFC Rutherford Appleton Laboratory, Chilton, Didcot, OX 11 0QX, UK

<sup>c</sup> Department of Life Sciences, University of Coimbra, Coimbra, Portugal

† Corresponding author

Electronic Supplementary Information (ESI) available: [details of any supplementary information available should be included here]. See DOI: 10.1039/x0xx00000x

equilibria induced by different media polarities were evaluated. In order to assist the assignment of the vibrational spectra, the N-deuterated species [ND<sub>2</sub>(CH<sub>2</sub>)<sub>3</sub>ND<sub>2</sub>] were prepared and analysed.

## Experimental

### Chemicals

1,3-diaminopropane (>99 %), 1,3-diaminopropane dihydrochloride (>98 %), carbon tetrachloride (99.9 %) and deuterium oxide (99.9 atom % D) were obtained from Sigma-Aldrich, (Sintra, Portugal).

The 1,3-dap-N-d<sub>4</sub> and [1,3-dap-N-d<sub>6</sub>]<sup>2+</sup>·2Cl<sup>-</sup> were prepared by repeatedly stirring (three times for ca. 1 h at room temperature) a mixture of either 1,3-dap-N-h<sub>4</sub> or [1,3-dap-N-h<sub>6</sub>]<sup>2+</sup>·2Cl<sup>-</sup> and D<sub>2</sub>O (ca. 10% excess), followed by distillation in a Büchi Vacuum Controller V-800 (50 mbar; 323 K). Purification of the samples was carried out shortly before running the spectra: the liquids were distilled under vacuum while the salts were recrystallized (sometimes repeatedly) from ethanol:water (1:1) (being obtained as white needles). Air or moisture sensitive samples (both the uncharged and the deuterated amines) were always kept on molecular sieves and handled in a glovebox, under a nitrogen or argon atmosphere.

### Vibrational spectra

**Raman spectroscopy.** The Raman spectra were obtained on a triple monochromator Jobin-Yvon T64000 Raman system (focal distance 0.640 m, aperture *f*/7.5) equipped with holographic gratings of 1800 grooves·mm<sup>-1</sup>. The premonochromator stage was used in the subtractive mode. The detection system was a liquid nitrogen cooled non-intensified 1024x256 pixel (1") Charge Coupled Device (CCD) chip. A Coherent (model Innova 300-05) Ar<sup>+</sup> laser was used as the light source, the output of which at 514.5 nm was adjusted to provide ca. 80 mW at the sample position. A 90° geometry, between the incident radiation and the collecting system, was employed. The entrance slit was set to 200 μm. An integration time of 3 s and 10-15 scans were used in all experiments.

In order to record the low-temperature Raman spectra of 1,3-dap and 1,3-dap-N-d<sub>4</sub> (240 K, solid phase) a home-made Harney-Miller type assembly was used, temperature monitored by the resistivity of a calibrated thermocouple.

Samples were sealed in Kimax glass capillary tubes of 0.8 mm inner diameter. Under the above mentioned conditions, the error in wavenumbers was estimated to be within 1 cm<sup>-1</sup>.

**FTIR spectroscopy.** The Fourier transform infrared (FTIR) spectra were recorded in a Bruker Optics Vertex 70 FTIR spectrometer purged by CO<sub>2</sub>-free dry air, in the 400-4000 cm<sup>-1</sup> range, using KBr disks (ca. 0.5% (w/w)). A Ge on KBr substrate beamsplitter and a liquid nitrogen cooled Mercury Cadmium Telluride (MCT) detector were used. The spectra were collected for 2 minutes (ca. 140 scans), at a 2 cm<sup>-1</sup> resolution, and the 3-term Blackman-Harris apodization function was applied. Under these conditions, the accuracy in wavenumbers was well below 1 cm<sup>-1</sup>.

**INS spectroscopy.** Inelastic Neutron Scattering is particularly useful for the study of this kind of hydrogenated compounds, yielding complementary information to that obtained from Raman and FTIR since it allows observation of some low frequency modes unavailable to the optical techniques. The neutron scattering cross-section of an atom ( $\sigma$ ) is characteristic of that atom and independent of its chemical environment, the value for hydrogen (80 barns) far exceeding that of all other elements (ca. 5 barns). Hence, the INS spectra is dominated by the vibrational modes involving a significant hydrogen displacement ( $u_i$ ), the intensity from a powdered sample at a energy  $\nu_i$  being represented by

$$S_i^*(Q, \nu_k) = \frac{(Q^2 u_i^2) \sigma}{3} \exp\left(-\frac{Q^2 \alpha_i^2}{3}\right) \quad (1)$$

where  $Q$  (Å<sup>-1</sup>) is the momentum transferred from the neutron to the sample and  $\alpha_i$  (Å) is associated with a weighted sum of all the displacements of the atom. Therefore, experimental data provide the energies of the vibrational transitions (the eigenvalues,  $\nu_i$ ) as well as the atomic displacements (the eigenvectors,  $u_i$ ). Additionally, the spectral intensities can be quantitatively compared with those DFT-calculated, allowing to relate molecular geometry (calculated results) with the experimental spectroscopic features, thus providing a reliable conformational insight of the system under study.

The INS spectra were obtained in the TOSCA spectrometer<sup>45,46</sup> at the ISIS Pulsed Neutron Source of the STFC Rutherford Appleton Laboratory (United Kingdom). This is an indirect geometry time-of-flight, high resolution (( $\Delta E/E$ ) ca. 1.25%), broad range spectrometer. The compounds (2 to 3 g for the solids and ca. 5 mL for the liquids) were placed in thin walled aluminium cans, which filled the beam (4x4 cm). To reduce the impact of the Debye-Waller factor (the exponential term in equation (1)) on the observed spectral intensity, the samples were cooled to cryogenic temperatures (ca. 10 K).

### Quantum mechanical calculations

The quantum mechanical calculations were carried out using the GAUSSIAN program package<sup>47</sup> within the Density Functional Theory (DFT) approach. The mPW1PW method, which comprises a modified version of the exchange term of Perdew-Wang and the Perdew-Wang 91 correlation functional<sup>48,49</sup> was used, along with the all-electron double-zeta split valence basis set 6-31G\*.<sup>50</sup>

All different permutation of skeletal dihedral angles – 60° (*gauche*, G), 180° (*trans*, T) or -60° (*gauche'*, G') – were considered in the definition of the starting geometries for optimization, which was performed without any symmetry constraints, with the following convergence criteria for the cutoffs of forces and step sizes: 0.000015 Hartree/Bohr for maximum force, 0.000010 Hartree/Bohr for root-mean-square force, 0.000060 Bohr for maximum displacement and 0.000040 Bohr for root-mean-square displacement.

The harmonic vibrational wavenumbers, as well as the Raman activities and infrared intensities, were obtained at the same theory level as the geometry optimization, in order to confirm

that the geometries correspond to a real minimum in the potential energy surface (no negative eigenvalues) as well as to estimate the zero-point vibrational energy (ZPVE) and the thermal corrections. The obtained wavenumber values were scaled according to Merrick *et al.*<sup>51</sup>: 0.9499 and 0.9828, respectively above and below 500 cm<sup>-1</sup>.

In order to simulate the pure liquid phase, and the aqueous and carbon tetrachloride solutions, self-consistent reaction field (SCRF) calculations were performed considering the tabulated dielectric constants at 25 °C ( $\epsilon=0.9$ , 78.39 and 2.228 for 1,3-DAP, H<sub>2</sub>O and CCl<sub>4</sub>, respectively). The polarisable continuum model (PCM) approach was used with the simple united atom topological model option (UA0) to set the atomic radii, as implemented in GAUSSIAN.<sup>47</sup>

Moreover, aiming at verifying the reliability of the conformational energy differences obtained with the mPW1PW/6-31G(d) method, both wB97XD<sup>52</sup> long-range-corrected and M06-2X<sup>53</sup> meta-hybrid functionals, in conjunction with the all-electron triple-zeta split valence (TZVP) basis set, were used. Additionally, energy single point calculations on the DFT optimised geometries using coupled cluster singles doubles (triple) [CCSD(T)]<sup>54</sup> (often considered as the computational chemistry “gold standard”), along with 6-311++G(2d,p), were performed.

## Results and discussion

### DFT Conformational Analysis

**H<sub>2</sub>N-CH<sub>2</sub>-CH<sub>2</sub>-CH<sub>2</sub>-NH<sub>2</sub>.** 1,3-diaminopropane can adopt different conformations, mainly by varying the dihedral angles around the N<sup>1</sup>-C<sup>4</sup>, C<sup>4</sup>-C<sup>7</sup>, C<sup>7</sup>-C<sup>10</sup> and C<sup>10</sup>-N<sup>13</sup> bonds (Figure 1).

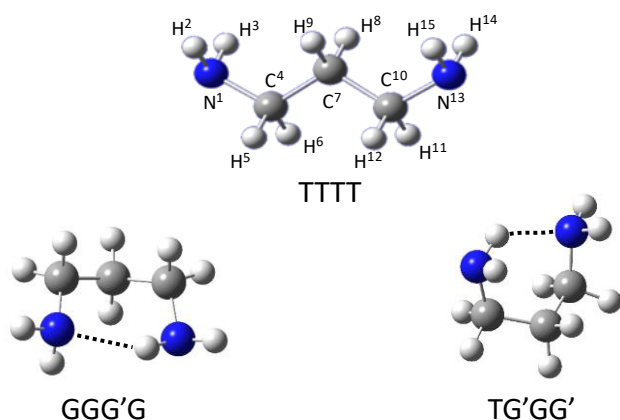


Figure 1-Schematic representation of some conformers of 1,3-diaminopropane.

Table 1 comprises the conformational energy differences, populations, thermochemical data and dipole moments obtained by DFT calculations, for twenty three conformations of this compound. The estimation of the  $\Delta E$ -based populations, assuming similar entropy contributions to the free energy of the distinct conformers, is not strictly correct since differences of up to 3.40 kJ mol<sup>-1</sup> were found for the entropy term ( $T\Delta S$ ). Thus,  $\Delta G$ -based populations at 298.15 K, calculated according to the Boltzmann law, are also presented in Table 1.

Conformations TGG'T and GGG'G' were not found to be potential energy surface minima, since some of their calculated

vibrational frequencies were imaginary (negative). Singularly, this result was only obtained for the isolated molecule, *ie.*, when solvent effects were considered, using the SCRF-PCM approach, these geometries were shown to be true energy minima (see below).

The most populated geometries were GGG'G (28%) and TG'GG' (20%), for which intramolecular (N)H...N hydrogen bonds can be established (Figure 1). The remaining conformers have calculated populations of less than 7%. Thus, it is possible to predict that the 1,3-dap gas phase system should contain different conformers in simultaneous equilibria with a predominance of the GGG'G and TG'GG' geometries.

The conformational stability of a molecule is influenced by various intramolecular effects, including steric, inductive, mesomeric, hyperconjugative, H-bonding and entropic interactions. For 1,3-dap it was found that the latter are particularly important (Table 1). Actually, the relative conformer populations taking into account the Gibbs energy leads to a slight population change: GGG'G (19.8%) and TG'GG' (15.2%), the remaining conformers accounting for 65% of the total population.

The decrease of the relative GGG'G and TG'GG' populations, when considering the Gibbs energy, is mainly due to the fact that the entropic component for these two conformations is much smaller than that calculated for all others, for which there is an additional stabilization resulting in positive  $T\Delta S$  values, above 1 kJ.mol<sup>-1</sup> (Table 1).

The reliability of these predictions was checked against the CCSD(T) gold standard approach, for the twelve most stable conformers (Table S1). It should be stressed that all the methodologies confirm the GGG'G as the lowest energy conformation. Despite this, there is no agreement on the ordering of conformational energy differences using different functionals. Furthermore, the root-mean-square deviations (RMSD) of  $\Delta E$  present lower values when wB97XD and M06-2X functionals with triple-zeta quality basis sets were used, but the RMSD of  $\Delta G$  obtained with the mPW1PW/6-31G(d) method displays the lowest value (Table S1). These findings support the claim of Padrão *et al.*<sup>14</sup> that mPW1PW/6-31G(d) are a suitable tool to study these kind of systems.

Table 2 presents the conformational energy differences, populations, thermochemical data and dipole moments for pure (liquid) 1,3-dap, obtained by SCRF-PCM calculations considering 298.15 K and the dielectric constant of the corresponding medium (in this case 1,3-dap itself).

Considering the energy values corrected for the zero-point vibrational energy (ZPVE), the most stable conformation in the condensed phase was found to be TTTT (Figure 1), with a predicted population of *ca.* 13% at 298 K. In fact, due to the small energy differences between conformers, the system under study should consist of a diversified mix at room temperature. Thus, the presence of the TTTG and TGTT conformers, which have the same energy, is also expected, with approximate populations of 11.5%. All other conformers have populations lower than 7.5% but, as they are in larger number, they are responsible for *ca.* 65% of the total population in the pure liquid phase (Table 2).

Table 1 - Calculated (mPW1PW/6-31G\*) conformational energies, populations (Pi), thermochemical data (at 298.15 K and 1 atm) and dipole moments ( $\mu$ ), for the 1,3-dap conformers.

| Conformer <sup>a</sup> | $s_i$ | $\Delta E$<br>(kJ.mol <sup>-1</sup> ) | $\Delta E_{ZPVE}^b$<br>(kJ.mol <sup>-1</sup> ) | $P_i(\Delta E_{ZPVE})^c$<br>(%) | $\Delta H$<br>(kJ.mol <sup>-1</sup> ) | $T\Delta S$<br>(kJ.mol <sup>-1</sup> ) | $\Delta G$<br>(kJ.mol <sup>-1</sup> ) | $P_i(\Delta G)^d$<br>(%) | $\mu^e$<br>(D) |
|------------------------|-------|---------------------------------------|--|---------------------------------|---------------------------------------|--|---------------------------------------|--------------------------|----------------|
| GGG'G                  | 2     | 0.00                                  | 0.00   | 28.0                            | 0.00                                  | 0.00                                   | 0.00                                  | 19.8                     | 1.80           |
| TG'GG'                 | 2     | 1.03                                  | 0.84   | 19.8                            | 0.96                                  | 0.32                                   | 0.64                                  | 15.2                     | 3.21           |
| TGGG'                  | 2     | 4.04                                  | 3.47   | 6.7                             | 3.90                                  | 1.61                                   | 2.30                                  | 7.7                      | 2.90           |
| TTTT                   | 1     | 5.39                                  | 3.57   | 3.2                             | 4.74                                  | 1.22                                   | 3.52                                  | 2.3                      | 2.04           |
| GGGG'                  | 2     | 4.28                                  | 4.32   | 4.7                             | 4.63                                  | 0.96                                   | 3.67                                  | 4.4                      | 1.76           |
| GG'G'G                 | 2     | 5.94                                  | 4.37   | 4.6                             | 5.17                                  | 2.06                                   | 3.11                                  | 5.5                      | 0.86           |
| TTGG'                  | 2     | 6.44                                  | 4.45   | 4.5                             | 5.50                                  | 2.94                                   | 2.56                                  | 6.9                      | 2.89           |
| TTTG                   | 2     | 6.65                                  | 4.67   | 4.1                             | 5.91                                  | 3.17                                   | 2.74                                  | 6.4                      | 1.77           |
| TGTT                   | 2     | 6.41                                  | 4.69   | 4.0                             | 5.65                                  | 2.61                                   | 3.04                                  | 5.6                      | 1.64           |
| GTGG'                  | 2     | 6.92                                  | 5.18   | 3.3                             | 6.13                                  | 2.57                                   | 3.57                                  | 4.5                      | 1.41           |
| TGTG                   | 2     | 7.25                                  | 5.54   | 2.8                             | 6.50                                  | 2.66                                   | 3.84                                  | 4.1                      | 1.80           |
| TGGT                   | 2     | 6.54                                  | 5.62   | 2.7                             | 6.20                                  | 0.12                                   | 6.09                                  | 1.6                      | 1.27           |
| GTTG                   | 2     | 8.20                                  | 6.25   | 2.1                             | 7.50                                  | 1.46                                   | 6.04                                  | 1.6                      | 1.46           |
| GTG'G                  | 2     | 8.28                                  | 6.39   | 2.0                             | 7.51                                  | 3.23                                   | 4.28                                  | 3.4                      | 1.63           |
| TTGG                   | 2     | 7.87                                  | 6.43   | 2.0                             | 7.40                                  | 2.60                                   | 4.80                                  | 2.7                      | 1.69           |
| TGTG'                  | 2     | 8.47                                  | 6.61   | 1.8                             | 7.63                                  | 2.88                                   | 4.75                                  | 2.8                      | 2.05           |
| GTTG'                  | 1     | 9.65                                  | 7.47   | 0.6                             | 8.79                                  | 3.40                                   | 5.39                                  | 1.1                      | 2.73           |
| TGGG                   | 2     | 9.52                                  | 7.57   | 1.2                             | 8.52                                  | 2.83                                   | 5.69                                  | 1.9                      | 1.90           |
| GTG'G'                 | 2     | 10.05                                 | 8.40   | 0.9                             | 9.49                                  | 2.96                                   | 6.53                                  | 1.3                      | 1.65           |
| GGTG                   | 2     | 10.92                                 | 9.04   | 0.7                             | 10.15                                 | 3.05                                   | 7.10                                  | 1.1                      | 2.68           |
| GGGG                   | 2     | 12.29                                 | 11.03  | 0.3                             | 11.92                                 | 1.15                                   | 10.77                                 | 0.2                      | 1.83           |
| TGG'T                  |       | 15.89                                 | 13.38  |                                 | 12.41                                 | -1.79                                  | 14.19                                 |                          | 1.17           |
| GGG'G'                 |       | 23.75                                 | 20.68  |                                 | 20.02                                 | -0.81                                  | 20.84                                 |                          | 2.67           |

<sup>a</sup> See Figure 1; <sup>b</sup>  $\Delta E_{ZPVE}$ , zero-point vibrational energy corrected relative energies; <sup>c</sup> population according to  $\Delta E_{ZPVE}$  values; <sup>d</sup> population according to  $\Delta G$  values; <sup>e</sup>  $1 \text{ D} = 1/3 \times 10^{-29} \text{ C m}$

When considering the population distribution based on Gibbs energies, this conformer mixture undergoes profound changes, being mostly comprised of TTTG (13.9%) and TGTT (13.1%) species, while the *all-trans* conformation (TTTT) becomes the fifth most populated one (7.5%). In fact, this conformer does not display the additional entropic stabilization that occurs in most other conformations which have a positive  $T\Delta S$  value (Table 2).

It should, however, be noted that the currently performed calculations only consider intermolecular interactions in the condensed phase in a global manner, through the dielectric constant of the medium, and do not take into account the specific nature of interactions such as intermolecular hydrogen bonds. In this perspective, the three-dimensional structure of the TTTT conformer will enable an interplay between the  $\text{NH}_2$  groups of the 1,3-dap molecules, *i.e.* the intermolecular connection of two adjacent molecules, much more easily than, for example, the GGG'G conformer (Figure 1; more stable in the gas phase) that has a non-linear geometry. In fact the formation of this type of intermolecular bonds is rendered much more difficult for the latter due to steric hindrance factors. The occurrence of intramolecular H-bonds, in turn, is not possible in both the TTTT, TTTG and TGTT conformers, thus favouring the intermolecular ones. The additional stabilization of the system caused by these close contacts can have profound implications in the corresponding conformational equilibria.

It should also be mentioned that, despite the pronounced changes in the conformational equilibrium due to the effect of the environment – gaseous vs. pure liquid – one cannot establish any correlation, either positive or negative, between the energy and dipole moment values for the distinct conformers.

For the simulation of the aqueous solution of 1,3-dap, when considering the population based on the electronic energy (ZPVE corrected), the conformational mixture is composed mainly by the TTTT (15.0%), TGTT (12.2%) and TTTG (12.0%) species. The remaining conformers, with populations below 8%, contribute with *ca.* 60% (Table S2) to the whole population. When the Gibbs energy is considered some differences are observed, the most prominent one being the decrease of the *all-trans* population, from 15.0% to 8.3% and the increase of conformers TTGG', from 7.6% to 9.6%, and TGGG', from 5.3% to 9.4%. The stabilization of the latter is due to a very high value of entropy ( $T\Delta S = 2.62 \text{ kJ mol}^{-1}$ ) when compared with the other conformers, in particular the TTTT (Table S2).

The water being a polar solvent, its polarity is prone to affect 1,3-dap's conformational stability. It would be expected that the conformations with a higher dipole moment would be favoured in aqueous solution. However this is not the case, the presence of conformations with an intermediate dipole moment ( $\approx 2.2 \text{ D}$ ) being preferred. As mentioned earlier, other effects than the dipole moment appear to be more relevant for determining the conformational stability of this system. Actually, once more no

correlation is found between the conformer energies and their calculated dipole moments (Table S2).

View Article Online  
DOI: 10.1039/C7NJ00810D

Table 2 - Calculated (mPW1PW/6-31G\*) conformational energies, populations (Pi), thermochemical data (at 298.15 K and 1 atm) and dipole moments ( $\mu$ ), for the 1,3-dap conformers in the pure liquid phase simulation (SCRFP-PCM)

| Conformer <sup>a</sup> | $s_i$ | $\Delta E$<br>(kJ.mol <sup>-1</sup> ) | $\Delta E_{zpv}$ <sup>b</sup><br>(kJ.mol <sup>-1</sup> ) | $P_i(\Delta E_{zpv})$ <sup>c</sup><br>(%) | $\Delta H$<br>(kJ.mol <sup>-1</sup> ) | $T\Delta S$<br>(kJ.mol <sup>-1</sup> ) | $\Delta G$<br>(kJ.mol <sup>-1</sup> ) | $P_i(\Delta G)$ <sup>d</sup><br>(%) | $\mu$ <sup>e</sup><br>(D) |
|------------------------|-------|---------------------------------------|--|---|---------------------------------------|--|---------------------------------------|-------------------------------------|---------------------------|
| GGG'G                  | 2     | 3.12                                  | 4.59   | 4.0                                       | 3.58                                  | -0.85                                  | 4.43                                  | 2.4                                 | 2.42                      |
| TG'GG'                 | 2     | 1.51                                  | 3.34   | 6.7                                       | 2.28                                  | -0.95                                  | 3.23                                  | 3.9                                 | 3.92                      |
| TGGG'                  | 2     | 3.35                                  | 3.78   | 5.5                                       | 3.46                                  | 2.25                                   | 1.22                                  | 9.0                                 | 3.48                      |
| TTTT                   | 1     | 0.00                                  | 0.00   | 13.2                                      | 0.00                                  | 0.00                                   | 0.00                                  | 7.5                                 | 2.55                      |
| GGGG'                  | 2     | 5.82                                  | 6.77   | 1.6                                       | 6.28                                  | 1.16                                   | 5.12                                  | 1.8                                 | 2.08                      |
| GG'G'G                 | 2     | 6.14                                  | 6.02   | 2.2                                       | 5.75                                  | 1.18                                   | 4.57                                  | 2.3                                 | 1.45                      |
| TTGG'                  | 2     | 3.36                                  | 3.06   | 7.5                                       | 2.99                                  | 1.91                                   | 1.08                                  | 9.5                                 | 3.54                      |
| TTTG                   | 2     | 2.27                                  | 2.02   | 11.4                                      | 2.07                                  | 1.90                                   | 0.17                                  | 13.9                                | 2.13                      |
| TGTT                   | 2     | 1.83                                  | 2.02   | 11.4                                      | 1.83                                  | 1.51                                   | 0.32                                  | 13.1                                | 1.97                      |
| GTGG'                  | 2     | 5.23                                  | 4.97   | 3.4                                       | 4.86                                  | 1.65                                   | 3.21                                  | 4.0                                 | 1.80                      |
| TGTG                   | 2     | 3.61                                  | 3.71   | 5.7                                       | 3.52                                  | 1.48                                   | 2.04                                  | 6.4                                 | 2.17                      |
| TGGT                   | 2     | 2.37                                  | 3.90   | 5.3                                       | 3.15                                  | -1.42                                  | 4.57                                  | 2.3                                 | 1.33                      |
| GTTG                   | 2     | 4.55                                  | 4.19   | 4.7                                       | 4.31                                  | 0.32                                   | 3.99                                  | 2.9                                 | 1.83                      |
| GTG'G                  | 2     | 6.30                                  | 5.93   | 2.3                                       | 5.93                                  | 2.13                                   | 3.81                                  | 3.1                                 | 1.98                      |
| TTGG                   | 2     | 4.38                                  | 4.73   | 3.7                                       | 4.51                                  | 1.30                                   | 3.21                                  | 4.0                                 | 2.00                      |
| TGTG'                  | 2     | 4.55                                  | 4.50   | 4.1                                       | 4.39                                  | 1.76                                   | 2.63                                  | 5.0                                 | 2.55                      |
| GTTG'                  | 1     | 5.23                                  | 4.75   | 1.9                                       | 4.92                                  | 2.20                                   | 2.72                                  | 2.4                                 | 3.41                      |
| TGGG                   | 2     | 6.08                                  | 6.10   | 2.1                                       | 5.88                                  | 1.68                                   | 4.20                                  | 2.6                                 | 2.44                      |
| GTG'G'                 | 2     | 7.10                                  | 7.13   | 1.4                                       | 7.04                                  | 1.69                                   | 5.36                                  | 1.6                                 | 2.10                      |
| GGTG                   | 2     | 6.92                                  | 6.93   | 1.5                                       | 6.81                                  | 1.58                                   | 5.23                                  | 1.7                                 | 3.36                      |
| GGGG                   | 2     | 9.00                                  | 9.80   | 0.5                                       | 9.43                                  | -0.40                                  | 9.82                                  | 0.3                                 | 2.32                      |
| TGG'T                  | 1     | 11.28                                 | 11.39  | 0.1                                       | 11.30                                 | 2.48                                   | 8.82                                  | 0.2                                 | 1.44                      |
| GGG'G'                 | 1     | 12.58                                 | 13.75  | 0.0                                       | 13.12                                 | 0.01                                   | 13.11                                 | 0.0                                 | 3.50                      |

<sup>a</sup> See Figure 1; <sup>b</sup>  $\Delta E_{zpv}$ , zero-point vibrational energy corrected relative energies; <sup>c</sup> population according to  $\Delta E_{zpv}$  values; <sup>d</sup> population according to  $\Delta G$  values; <sup>e</sup> 1 D =  $1/3 \times 10^{-2}$  C m

In turn, for the 1,3-dap/CCl<sub>4</sub> solution it is possible to forecast the existence of two conformations with higher stability, TG'GG' (14,6%) and GGG'G (13,8%) (Table S3; Figure 1). Nevertheless, there are drastic differences in this conformational equilibrium when the populations are determined considering the Gibbs energy values: six conformers with populations between 8.7 and 10.5% (TTTT, TG'GG', TGTT, TGGG', GGG'G and TTGG'; Table S3). Note that the most populated conformations considering  $\Delta E_{zpv}$  (TG'GG' and GGG'G) show negative entropy values ( $\Delta S$ ), *i.e.* in these two conformers the entropic factor plays a destabilising role. Conversely, for conformers TTTG, TGTT, TGGG' and TTGG' the  $T\Delta S$  value is higher than 2.0 kJ.mol<sup>-1</sup>, which results in an additional stability and very low  $\Delta G$  values. Since carbon tetrachloride is non-polar, it would be expected that the most stable conformations adopted by 1,3-dap in CCl<sub>4</sub> solution were the less polar ones. Instead, the opposite was observed: three of the most stable conformations display the largest dipole moment values (> 3.1 Debye). This evidences that, once again, the dipole moment is not a decisive parameter in the conformational equilibrium of this system.

Table S4 contains the structural parameters for the most stable conformations in each media considered in the present work. It is possible to conclude that, for the same conformation but different chemical environments, the differences between

bond lengths, angles and dihedral angles are negligible. There are no experimental values reported in the literature (X-ray diffraction, neutron diffraction, etc.) for a comparison with the values presently obtained. It is believed, however, that there are good estimates for real systems insofar as the methodology has proven very effective in other systems.<sup>14,43</sup>

**[H<sub>3</sub>N-CH<sub>2</sub>-CH<sub>2</sub>-CH<sub>2</sub>-NH<sub>3</sub>]<sup>2+</sup>.** Table 3 presents the conformational energy differences, populations, thermochemical data and dipole moments obtained for different conformations of the 1,3-dap N-ionised derivative ([1,3-dap-N-h<sub>6</sub>]<sup>2+</sup>). Since both amine groups are protonated (NH<sub>3</sub><sup>+</sup>), the hydrogen atoms bound to nitrogen are rendered equivalent. Therefore, the conformational analysis becomes much simpler, the number of possible conformations with minimal energy being drastically decreased. In fact, only three conformers were found, one being much more stable than the others: the *all-trans* conformer (TT) with a population predicted to be *ca.* 99%.

Table 3 - Calculated (mPW1PW/6-31G\*) conformational energies, populations (Pi), thermochemical data (at 298.15 K and 1 atm) and dipole moments ( $\mu$ ), for the  $[H_3N-CH_2-CH_2-CH_2-NH_3]^{2+}$  conformers.

| Conformer | $s_i$ | $\Delta E_{zpv}^a$<br>(kJ.mol <sup>-1</sup> ) | $P_i(\Delta E_{zpv})^b$<br>(%) | $\Delta H$<br>(kJ.mol <sup>-1</sup> ) | $T\Delta S$<br>(kJ.mol <sup>-1</sup> ) | $\Delta G$<br>(kJ.mol <sup>-1</sup> ) | $P_i(\Delta G)^c$<br>(%) | $\mu^d$<br>(D) |
|-----------|-------|---|--------------------------------|---------------------------------------|--|---------------------------------------|--------------------------|----------------|
| TT        | 1     | 0,00  | 99,6                           | 0,00                                  | 0,00                                   | 0,00                                  | 98,9                     | 1,36           |
| TG        | 2     | 14,83   | 0,4                            | 14,87                                 | 2,24                                   | 12,63                                 | 1,1                      | 2,18           |
| GG        | 2     | 27,09   | 0,0                            | 27,48                                 | 3,37                                   | 24,10                                 | 0,0                      | 1,64           |

<sup>a</sup>  $\Delta E_{zpv}$ , zero-point vibrational energy corrected relative energies; <sup>b</sup> population according to  $\Delta E_{zpv}$  values; <sup>c</sup> population according to  $\Delta G$  values; <sup>d</sup>  $D = 1/3 \times 10^{-2}$  C m

### Vibrational analysis

**H<sub>2</sub>N-CH<sub>2</sub>-CH<sub>2</sub>-CH<sub>2</sub>-NH<sub>2</sub>.** Figure 2 comprises the Raman and FTIR spectra for liquid (pure) 1,3-dap, whereas Figure 3 represents the Raman and INS spectra for its solid phase.

The experimental wavenumbers are presented in Table 4, along with the DFT calculated values for the TTTT conformer (C<sub>2v</sub> symmetry). In this conformation the molecule displays 39 normal vibrational modes distributed by four symmetry species, as follows: 12A<sub>1</sub> + 8A<sub>2</sub> + 9B<sub>1</sub> + 10B<sub>2</sub>. All these vibrations are Raman- and INS-active, whereas only 31 fundamental modes are expected on the infrared spectra as the eight A<sub>2</sub> vibrations are IR-inactive. Actually, INS being a non-optical vibrational technique it is not subject to the optical selection rules.

The agreement between the experimental and calculated wavenumbers, after scaling according to Merrick *et al.*<sup>51</sup>, was found to be rather good (Figure S1). In fact, since the calculated energy differences between the five most stable conformers

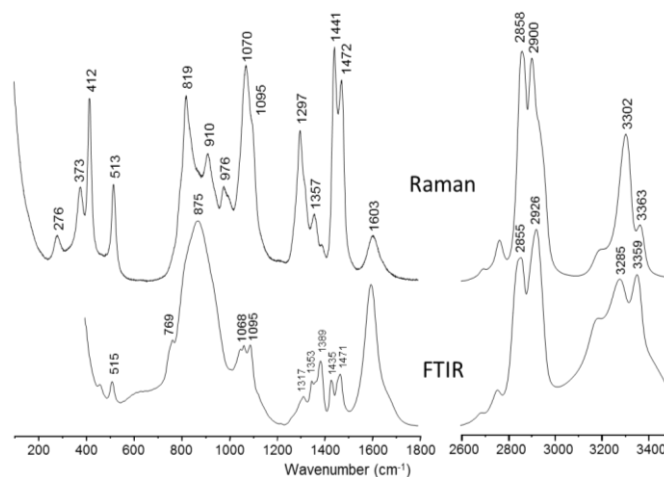


Figure 2- Raman (100-1800 and 2600-3500 cm<sup>-1</sup>) and FTIR (400-1800 and 2600-3500 cm<sup>-1</sup>) spectra of 1,3-diaminopropane in the liquid phase.

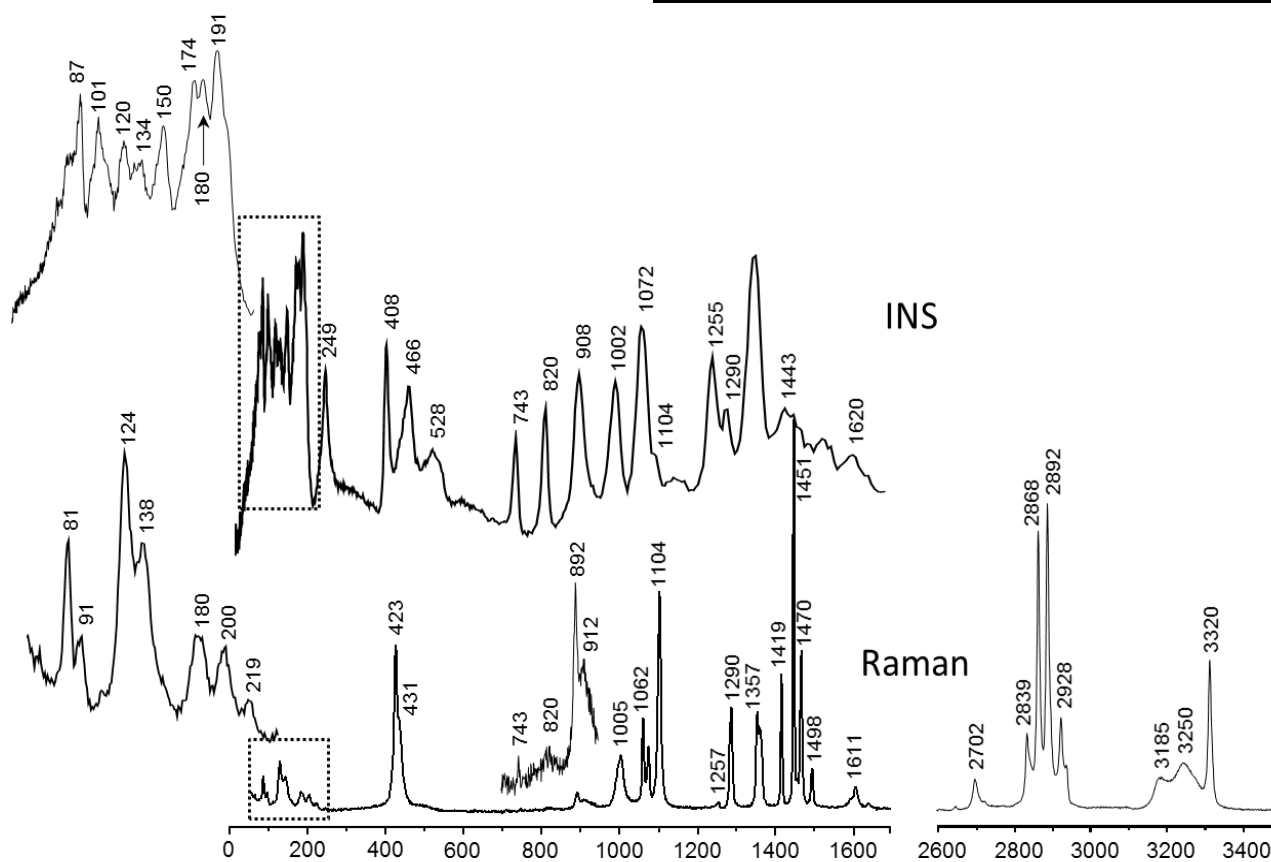


Figure 3 - INS (0-1700 cm<sup>-1</sup>) and Raman (50-1700 cm<sup>-1</sup>) spectra of 1,3-diaminopropane in the solid phase.



does not exceed *ca.* 1 kJ mol<sup>-1</sup>, all of these conformers are significantly populated at room temperature (Table 2). However, the calculated values for the low frequency region (below 600 cm<sup>-1</sup>), which is the most conformationally sensitive one, are remarkably consistent with the sole presence of conformer TTTT for the solid 1,3-dap. Table 4 also contains the complete assignment of 1,3-dap experimental bands to the normal modes of vibration. It is worthwhile to mention that most of the observed frequencies can be considered as group frequencies, *i.e.* highly localized on a particular group within the molecule.

A full assignment of the vibrational spectra was carried out considering both nondeuterated and N-deuterated samples, as the deuteration clearly evidences which bands correspond to vibrations of the NH<sub>2</sub> groups: i) in the 3150-3400 cm<sup>-1</sup> region, the NH<sub>2</sub> symmetric ( $\nu_s$ ) and antisymmetric ( $\nu_{as}$ ) stretching vibrations (Figures 2 and 3), that are detected at 2350-2550 cm<sup>-1</sup> for 1,3-dap-N-d<sub>4</sub> (Figure 4), displaying the expected wavenumber red shift of *ca.* 1.37x; ii) the scissoring modes of the amine groups ( $\alpha$ NH<sub>2</sub>) at *ca.* 1600 cm<sup>-1</sup> (Figure 2), that deviate to *ca.* 1197 cm<sup>-1</sup> upon deuteration (Figure 4); iii) the NH<sub>2</sub> twisting at 1353 cm<sup>-1</sup> (Figure 2), which are observed at 1153 cm<sup>-1</sup> for the deuterated compound (Figure 4); iv) the FTIR broad and intense NH<sub>2</sub> wagging at 875 cm<sup>-1</sup> (Figure 2), that is downward shifted (by *ca.* 100 cm<sup>-1</sup>) in the ND<sub>2</sub> counterpart (Figure 4); and v) the amine torsion at 431 cm<sup>-1</sup>, detected as a shoulder of the longitudinal acoustic mode 1 (LAM1) in the Raman spectrum of solid 1,3-dap (Figure 3), that emerges as a weak but well defined Raman band at 324 cm<sup>-1</sup> in solid 1,3-dap-N-d<sub>4</sub> (Figure 4).

As expected, vibrational modes not directly related with the amine groups do not show comparable wavenumber shifts upon deuteration. However, there are some interesting deviations in the low wavenumber region that should be mentioned. In particular, the bands at 513, 412 and 373 cm<sup>-1</sup> in the Raman spectrum of liquid 1,3-dap (Figure 2), assigned to NCC skeletal deformations, display small displacements to lower wavenumbers in the 1,3-dap-N-d<sub>4</sub> spectrum (23, 14 and 14 cm<sup>-1</sup>, respectively). Actually, the nitrogen atoms involved in the  $\delta$ NCC modes are linked to deuterium atoms, so that the amine group, considered as a whole, has a greater mass (18 instead of 16 u). Thus, while the force constant remains equal, since it is the same vibrational mode, there is a displacement of the bands due to a mass effect.

The amine wagging vibrations, in turn, are particularly interesting, as they are highly sensitive to the increase of hydrogen bond type interactions in the solid phase<sup>3</sup>: an upward shift of *ca.* 30 cm<sup>-1</sup> is observed when going from the liquid to the solid, from *ca.* 875 to *ca.* 905 cm<sup>-1</sup> (Figures 2 and 3). This vibrational mode, extremely weak in the Raman spectrum, is clearly observed by INS at 908 cm<sup>-1</sup> (Figure 3). A similar shift is observed by Raman for the ND<sub>2</sub> wagging mode with A<sub>1</sub> symmetry, at 803 and 830 cm<sup>-1</sup> for the liquid and solid samples, respectively (Figure 4). An analogous shift in both the nondeuterated and N-deuterated molecules, *i.e.* an equivalent change in the corresponding force constants, reveals that hydrogen bond type and deuterium bond type interactions have the same magnitude.

Analysis of the INS spectrum of 1,3-dap (Figure 3) allows to observe signals not available to the optical techniques (Raman and FTIR). Firstly, the bands corresponding to the longitudinal and transversal acoustic modes (LAM and TAM, respectively), previously assigned by the authors,<sup>24,25</sup> are only detectable by INS (excluding LAM1 which is also observed in Raman). Also the INS signal at 743 cm<sup>-1</sup>, ascribed to CH<sub>2</sub> rocking, is hardly seen in the Raman spectrum (Figure 3). These observations are not surprising, since the vibrational techniques currently used are based on different physical processes: light scattering vs neutron diffraction.

Regarding the Raman signals at 373/359 and 513/490 cm<sup>-1</sup>, detected for the pure liquids (nondeuterated/N-deuterated, Figures 2 and 4), there are completely absent from the solid phase spectra (Figures 3 and 4). Actually, there is a fairly good correspondence between the  $\delta$ NCCCN values predicted for the *all-trans* geometry and the ones that remain on the solid phase vibrational spectra, which allow to conclude that only the TTTT conformer is present in the solid sample, while the liquid consists of simultaneous equilibria of different conformers. In fact, when a *gauche* geometry around one of the CC bonds is considered, the skeletal deformation modes are predicted to be at 351 and 504 cm<sup>-1</sup> (calculated values for the TGTT geometry), in close agreement with the band wavenumbers that disappear in the liquid→solid transition. It should be emphasized that the five most stable conformers (TTTT, TTTG, TGTT, TTGG' and TGGG') account for 53% of the liquid phase population (Table 2).

**Solvent effect.** In order to access the influence of environment polarity on the liquid 1,3-dap conformational equilibria, solutions of this diamine in both a polar solvent (water) and an apolar one (carbon tetrachloride) were prepared and the Raman spectra were recorded. Moreover, different molar fractions amine/solvent were used, to evaluate possible concentration effects.

Regarding the aqueous solutions (Figure S2) some small changes could be observed upon dilution: i) a 9 cm<sup>-1</sup> upward shift of the  $\delta$ NCC mode at 373 cm<sup>-1</sup>, assigned to an increased preference for a *gauche* arrangement around one of the CC skeletal bonds; ii) the narrowing of the amine groups relating bands at 1603 and 3302 cm<sup>-1</sup>, probably due to a lower conformational dispersion; and iii) the apparent intensity decrease of the 910 cm<sup>-1</sup> band, owing to the narrowing/downward shift of the NH<sub>2</sub> wagging mode that occurs in the same region and is clearly detected for both liquid (by FTIR, at 875 cm<sup>-1</sup>) and solid samples (by Raman, at 892 cm<sup>-1</sup>) spectra. A progressive shift to higher wavenumbers ( $\leq$  15 cm<sup>-1</sup>) of the CH<sub>2</sub> symmetric and antisymmetric stretching bands with increasing molar fractions of water was also detected, due to the solvent polarity (Figure 5). In fact, it is known that these stretching modes are sensitive to interchain interactions and to the polarity of the environment.<sup>1,11,18</sup> The observed Raman blue shift exposes a hydrophobic repulsive effect of water on the hydrophobic methylene groups of 1,3-dap,<sup>17</sup> which lead to an additional stabilization of the conformers with a *gauche* arrangement of the alkyl chain.

Table 4 - Vibrational (FTIR, Raman and INS) experimental and DFT-calculated harmonic wavenumbers (cm<sup>-1</sup>) for 1,3-diaminopropane and its N-deuterated derivative, in the liquid and solid states.

View Article Online  
DOI: 10.1039/C7NJ00810D

| Experimental |       |                         |       | Calculated <sup>a</sup> |       |       | Tentative assignment <sup>b</sup> |                |   |
|--------------|-------|-------------------------|-------|-------------------------|-------|-------|-----------------------------------|----------------|---|
| 1,3-DAP      |       | 1,3-DAP-ND <sub>4</sub> |       |                         |       |       |                                   |                |   |
| Liquid       | Solid | Liquid                  | Solid |                         |       |       |                                   |                |   |
| FTIR         | Raman | Raman                   | INS   | FTIR                    | Raman | Raman |                                   |                |   |
| —            |       | 81                      | 77    | —                       |       | 80    | —                                 | External mode  |   |
| —            |       | 91                      | 87    | —                       |       | 92    | —                                 | External mode  |   |
| —            |       | 107                     | 101   | —                       |       | —     | —                                 | External mode  |   |
| —            |       | 124                     | 120   | —                       |       | 124   | —                                 | External mode  |   |
| —            |       | 138                     | 134   | —                       |       | 139   | —                                 | External mode  |   |
| —            |       |                         | 150   | —                       |       | —     | —                                 | External mode  |   |
| —            |       | 180                     | 174   | —                       |       | 172   | 120                               | B <sub>1</sub> | δ CCN (out-of-plane; TAM2)                                |
| —            |       | 200                     | 180   | —                       |       | 190   | 123                               | A <sub>2</sub> | δ CCN (out-of-plane; TAM1)                                |
| —            |       | 219                     | 191   | —                       |       | 209   | —                                 | —              |   |
| —            |       |                         | ~199  | —                       |       | —     | —                                 | —              |   |
| —            |       |                         | 249   | —                       |       | —     | 180                               | A <sub>1</sub> | δ NCCN (in-plane; LAM3)                                   |
| —            | 276   |                         |       | —                       | 271   |       | —                                 | —              |   |
| —            |       |                         |       | —                       |       | 324   | —                                 | A <sub>2</sub> | τ ND <sub>2</sub>   |
| —            | 373   |                         |       | —                       | 359   |       | —                                 | —              | δ NCC   |
| —            | 412   | 423                     | 408   | —                       | 398   | 411   | 395                               | A <sub>1</sub> | δ NCCN (in-plane; LAM1)                                   |
|              |       | 431                     | ~440  | —                       |       |       | 298                               | A <sub>2</sub> | τ NH <sub>2</sub>   |
| 463          |       |                         | 466   | —                       |       |       | 438                               | B <sub>2</sub> | δ NCCN (in-plane; LAM2)                                   |
| 515          | 513   |                         |       | —                       |       | 490   | —                                 | —              | δ CCC + δ NCC   |
|              |       |                         | 528   | —                       |       |       | —                                 | —              | τ NH <sub>2</sub> (H-bonded)                              |
|              |       |                         |       | 723                     |       | 718   | —                                 | B <sub>2</sub> | 324+411   |
|              |       |                         |       |                         |       | 736   | —                                 | —              | ω ND <sub>2</sub>   |
| 769          | ~770  | 743                     | 743   | ~765                    | 768   | 748   | 714                               | B <sub>1</sub> | ρ CH <sub>2</sub>   |
|              |       |                         |       |                         | 803   | 830   | —                                 | A <sub>1</sub> | ω ND <sub>2</sub>   |
|              |       |                         |       | ~830                    | 834   |       | —                                 | —              | ω ND <sub>2</sub>   |
|              | 819   | 820                     | 820   |                         |       |       | 788                               | A <sub>2</sub> | ρ CH <sub>2</sub> + t CH <sub>2</sub> + t NH <sub>2</sub> |
| 875          |       | 892                     | 908   |                         |       |       | 888                               | B <sub>2</sub> | ω NH <sub>2</sub>   |
|              |       | 912                     |       |                         |       |       | 875                               | A <sub>1</sub> | ω NH <sub>2</sub>   |
|              | 910   |                         |       |                         | 915   |       | —                                 | —              | v CC  |
|              |       |                         |       |                         | 947   |       | —                                 | —              | v CC  |
|              |       |                         |       |                         |       |       | 954                               | B <sub>1</sub> | t CH <sub>2</sub> + t NH <sub>2</sub>                     |
|              | 976   | 1005                    | 1002  | 979                     | 984   | 996   | 995                               | B <sub>2</sub> | v <sub>a</sub> CC (+ ω NH <sub>2</sub> )                  |
|              |       |                         |       | 1019                    | 1019  |       | —                                 | —              | v CC  |
|              |       |                         |       | ~1035                   | 1039  | 1039  | —                                 | —              | v CC  |
| 1068         | 1070  | 1062                    | 1072  | 1066                    | 1070  | 1060  | 1044                              | A <sub>1</sub> | v <sub>s</sub> CC   |
|              |       | 1076                    |       |                         |       | 1072  | 1057                              | B <sub>2</sub> | v <sub>a</sub> CN + v <sub>a</sub> CC                     |
| 1095         | 1095  | 1104                    | 1104  | 1097                    | 1099  | 1084  | 1104                              | A <sub>1</sub> | v <sub>s</sub> CN   |
|              |       |                         |       |                         | 1153  |       | —                                 | —              | t ND <sub>2</sub>   |
|              |       |                         |       | 1197                    | 1196  | 1213  | —                                 | —              | α ND <sub>2</sub>   |
|              |       |                         |       | ~1235                   | 1243  |       | —                                 | —              | t CH <sub>2</sub>   |
|              |       | 1257                    | 1255  | ~1270                   | 1276  |       | 1238                              | B <sub>2</sub> | ω CH <sub>2</sub> + t CH <sub>2</sub>                     |
|              | 1297  | 1290                    | 1290  | 1300                    | 1305  | 1309  | 1276                              | A <sub>2</sub> | t CH <sub>2</sub>   |
| 1317         |       |                         |       | 1321                    |       |       | —                                 | —              |   |
| 1353         | 1357  | 1357                    |       |                         |       |       | 1338                              | A <sub>1</sub> | t NH <sub>2</sub> + t CH <sub>2</sub>                     |
| 1389         | 1390  | 1364                    | 1364  | 1369                    | 1373  | 1368  | 1355                              | B <sub>2</sub> | ω CH <sub>2</sub>   |
|              |       | 1419                    |       |                         |       | 1419  | —                                 | —              | α CH <sub>2</sub>   |
| 1435         | 1441  | 1451                    | 1443  | 1442                    | 1445  | 1450  | 1428                              | A <sub>1</sub> | α CH <sub>2</sub>   |
| 1471         | 1472  | 1470                    |       | 1471                    | 1479  | 1475  | 1455                              | A <sub>1</sub> | α CH <sub>2</sub>   |
|              |       | 1498                    |       |                         |       |       | —                                 | —              |   |
|              |       |                         |       | 1554                    |       |       | —                                 | —              | α NHD   |
| 1601         |       |                         |       |                         |       |       | 1598                              | B <sub>2</sub> | α NH <sub>2</sub>   |

|       |       |       |  |      |      |       |                |   |  |
|-------|-------|-------|--|------|------|-------|----------------|---|--|
| 1603  | 1611  | 1620  |  |      |      | 1599  | A <sub>1</sub> | $\alpha$ NH <sub>2</sub>                  | View Article Online<br>DOI: 10.1039/C7NJ00810D |
|       |       |       |  | 2366 | 2370 | 2358  |                | v <sub>s</sub> ND <sub>2</sub> (D bonded) |  |
|       |       |       |  | 2424 | 2434 | 2431  |                | v <sub>s</sub> ND <sub>2</sub>            |  |
|       |       |       |  | 2506 | 2511 | 2483  |                | v <sub>a</sub> ND <sub>2</sub>            |  |
| ~2690 | ~2690 | 2702  |  |      | 2722 | 2718  |                | Overtone or combination mode              |  |
| 2760  | 2760  |       |  |      | 2755 |       |                | Overtone or combination mode              |  |
|       |       | 2839  |  |      |      | ~2845 | 2882           | A <sub>1</sub>                            | v <sub>s</sub> CH <sub>2</sub>                 |
| 2855  | 2858  | 2868  |  | 2864 | 2871 | 2871  | 2904           | A <sub>1</sub>                            | v <sub>s</sub> CH <sub>2</sub>                 |
|       |       | 2892  |  |      |      | 2893  | 2917           | B <sub>1</sub>                            | v <sub>a</sub> CH <sub>2</sub>                 |
| 2926  | 2900  | 2928  |  | 2933 | 2911 | 2930  | 2953           | B <sub>1</sub>                            | v <sub>a</sub> CH <sub>2</sub>                 |
|       | ~2930 |       |  |      |      | 2955  |                |   | v <sub>a</sub> CH <sub>2</sub>                 |
| ~3190 | 3190  | ~3185 |  |      |      |       |                |   | v <sub>s</sub> NH <sub>2</sub> (H bonded)      |
| 3285  | 3302  | ~3250 |  |      |      |       | 3263           |   | v <sub>s</sub> NH <sub>2</sub>                 |
| 3359  | 3363  | 3320  |  |      |      |       | 3341           |   | v <sub>a</sub> NH <sub>2</sub>                 |

<sup>a</sup> For the TTTT conformer (C<sub>2v</sub> symmetry) of 1,3-diaminopropane at mPW1PW/6-31G\* level within SCRF approach: calculated values scaled according to Merrick *et al.* [45]: 0.9499 and 0.9828, above and below 500 cm<sup>-1</sup>, respectively. <sup>b</sup> Abbreviations:  $\delta$ , deformation;  $\tau$ , torsion;  $\omega$ , wagging; t, twisting;  $\rho$  - rocking;  $\alpha$ , scissoring; v, stretching; s, symmetric; a, antisymmetric; TAM, Transverse Acoustic Mode; LAM, Longitudinal Acoustic Mode.

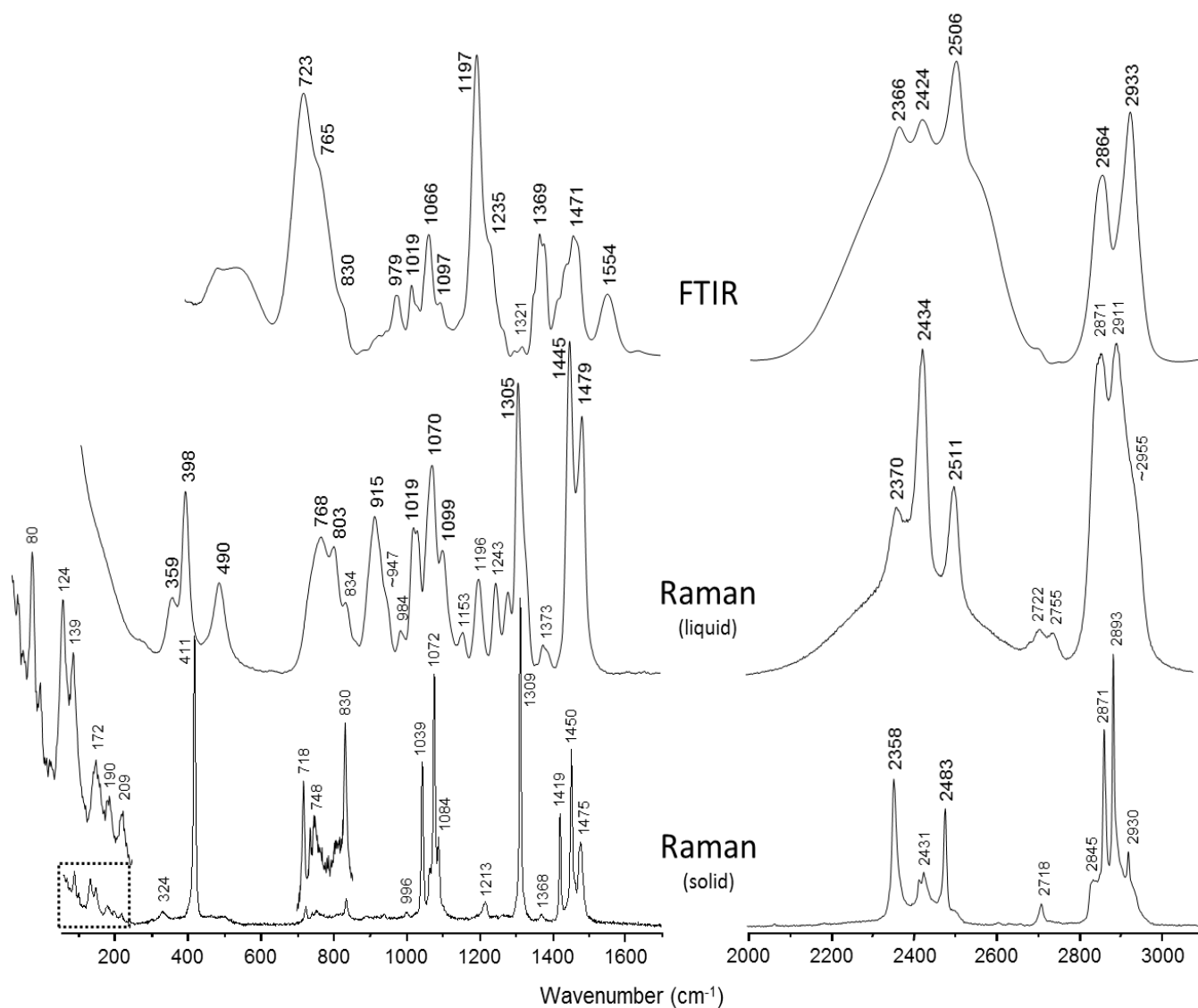


Figure 4 - FTIR (400-1700 and 2000-3100 cm<sup>-1</sup>) and Raman (100-1700 and 2000-3100 cm<sup>-1</sup>) spectra of 1,3-diaminopropane-N-d<sub>4</sub> in the liquid phase. Raman (50-1700 and 2000-3100 cm<sup>-1</sup>) spectrum of 1,3-diaminopropane-N-d<sub>4</sub> in the solid phase.

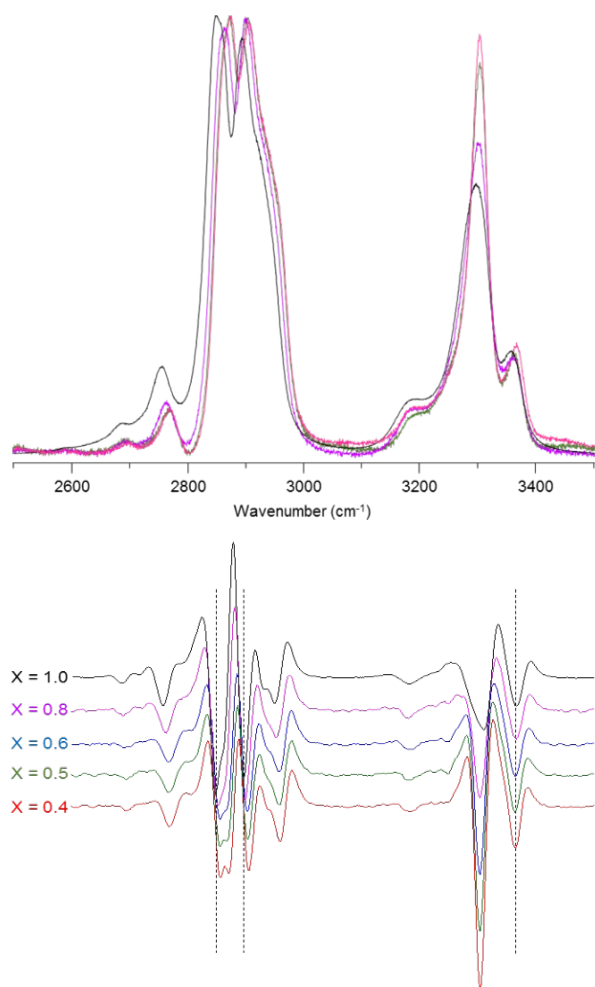


Figure 5 -Raman spectra (2500-3500 cm<sup>-1</sup>) (upper) and second derivative (bottom) of 1,3-diaminopropane aqueous solution, at different molar fractions.

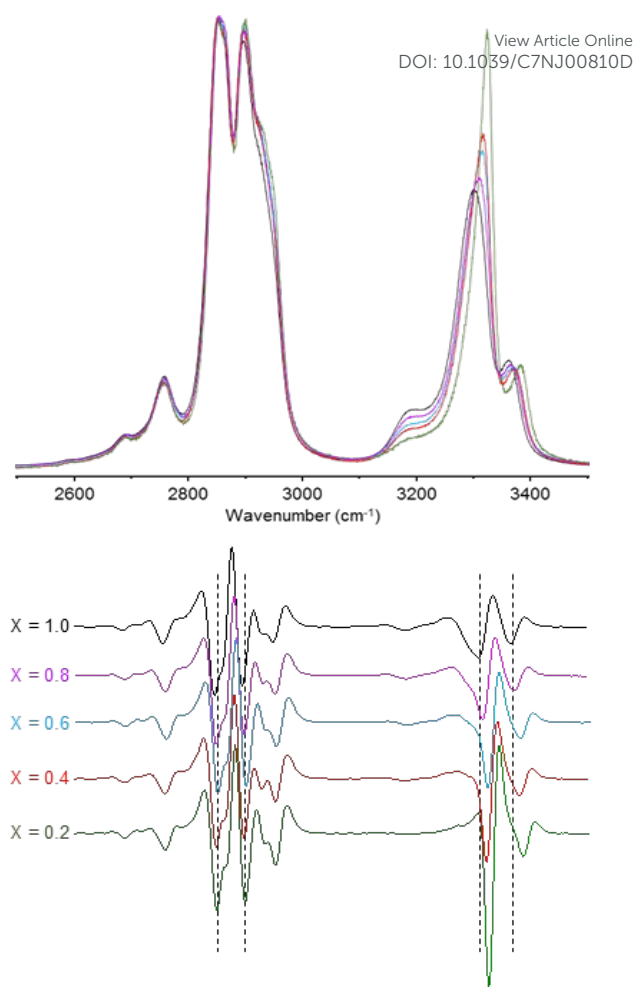


Figure 6 - Raman spectra (2500-3500 cm<sup>-1</sup>) (upper) and second derivative (bottom) of 1,3-diaminopropane/CCl<sub>4</sub> solution, at different molar fractions.

Concerning the carbon tetrachloride solutions (Figure S3), the vibrational bands from the solvent hinder a clear observation of the solute signals and do not allow to determine any intensity changes in the 350-550 cm<sup>-1</sup> range. However, the bands seem not to be affected by dilution in this apolar solvent. Interestingly enough, the appearance of a new 1,3-dap band upon dilution at 877 cm<sup>-1</sup> can be assigned to a change in conformational equilibrium, particularly to the presence of conformers not detected in the pure liquid. In the higher wavenumber region, in turn, there is an opposite behaviour to the one detected in aqueous solution: the methylene stretching signals do not undergo significant changes, while the amine stretching bands experience both a blue shift and an intensity enhancement with increasing dilution (Figure 6). Moreover, a simultaneous intensity decrease of the 3200 cm<sup>-1</sup> band, which is assigned to the  $\nu_s\text{NH}_2$  mode when the amine group is involved in hydrogen bond type close contacts, is observed (Figure 6). In fact, when the CCl<sub>4</sub> molar fraction is increased, 1,3-dap molecules "not connected", *i.e.* not involved in H-bonds (neither intra- nor intermolecular) are predominant.

**[H<sub>3</sub>N-CH<sub>2</sub>-CH<sub>2</sub>-CH<sub>2</sub>-NH<sub>3</sub>]<sup>2+</sup>.** Figure 7 comprises Raman, FTIR and INS spectra for [H<sub>3</sub>N-CH<sub>2</sub>-CH<sub>2</sub>-CH<sub>2</sub>-NH<sub>3</sub>]<sup>2+</sup>·2Cl<sup>-</sup> while Figure 8 represents the spectra for the N-deuterated molecule. Experimental wavenumbers are presented in Table 5, along with the DFT calculated values for the TT conformer (C<sub>2v</sub> symmetry), the hegemonic configuration (99 %, Table 3). For the solid samples, the occurrence of intermolecular interactions has a pronounced effect on the vibrational spectra. This is particularly important when amine systems are targeted, as they are prone to form extensive intermolecular hydrogen bond networks. By neglecting the effect of those interactions, significant deviations between the calculated and the experimental data are frequently observed. Not surprisingly, the vibrational modes that are mostly affected concern the terminal -NH<sub>3</sub><sup>+</sup> groups as they are directly involved in intermolecular interactions. Among the 18 related modes, the most affected are, as previously found,<sup>55,56</sup> the stretching modes ( $\nu_s\text{NH}_3$  and  $\nu_{as}\text{NH}_3$ ) and the two torsional vibrations ( $\tau\text{NH}_3$ ). These were found to be downward and upward shifted, respectively, by more than 300 cm<sup>-1</sup>, due to N-H...Cl interactions. The effect on the deformation modes ( $\delta_s\text{NH}_3$  and  $\delta_{as}\text{NH}_3$ ) are comparatively insignificant, with an upward shift of less than 50 cm<sup>-1</sup>. The NH<sub>3</sub><sup>+</sup> rocking modes ( $\rho\text{NH}_3$ ), on the other hand, are slightly more affected than  $\delta\text{NH}_3$ , with a negligible

blue shift as compared to the  $\nu\text{NH}_3$  and  $\tau\text{NH}_3$  modes (between 56 and 86  $\text{cm}^{-1}$ ). Besides the  $-\text{NH}_3^+$ -related modes, only one other type of fundamental vibrations was found to be considerably affected by the presence of  $\text{N-H}\cdots\text{Cl}$  interactions: the two NC stretching modes ( $\nu_{\text{asNC}}$  and  $\nu_{\text{sNC}}$ ) were found to be upward shifted by more than 150  $\text{cm}^{-1}$ , probably as a consequence of the proximity of the N-C bond to the  $\text{N-H}\cdots\text{Cl}$  contacts.

As a consequence of the significant shifts promoted by  $\text{N-H}\cdots\text{Cl}$  close contacts, several changes were observed in the relative

ordering of the vibrational modes. If these are not considered, the assignment of the experimental vibrational spectra are inaccurate. A reported vibrational spectroscopic analysis of 1,2-ethylenediamine dihydrochloride ( $[\text{H}_3\text{N}(\text{CH}_2)_2\text{NH}_3]^{2+}\cdot 2\text{Cl}^-$ )<sup>55</sup> allowed to conclude that an precise theoretical forecast of the vibrational frequencies requires a molecular adduct comprising one cation surrounded by six chloride counterions, in a crystal structure based arrangement. However, such a molecular model tends to become too computationally expensive as the diamine size increases.

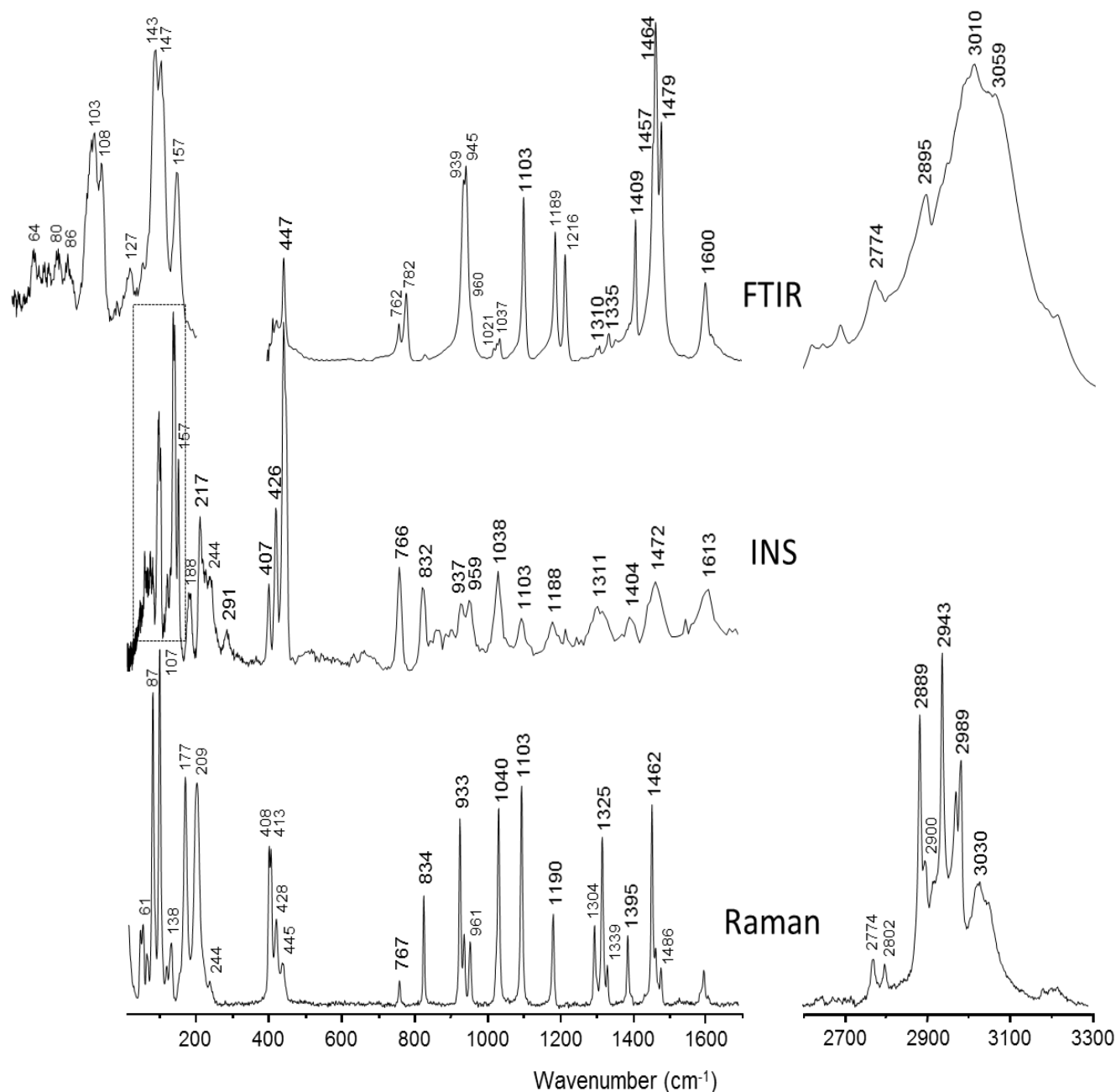


Figure 7 - FTIR (400-1700 and 2600-3300  $\text{cm}^{-1}$ ), INS (0-1700  $\text{cm}^{-1}$ ) and Raman (10-1700 and 2600-3300  $\text{cm}^{-1}$ ) spectra of solid 1,3-diaminopropane- $\text{N-h}_6^{2+}\cdot 2\text{Cl}^-$ .

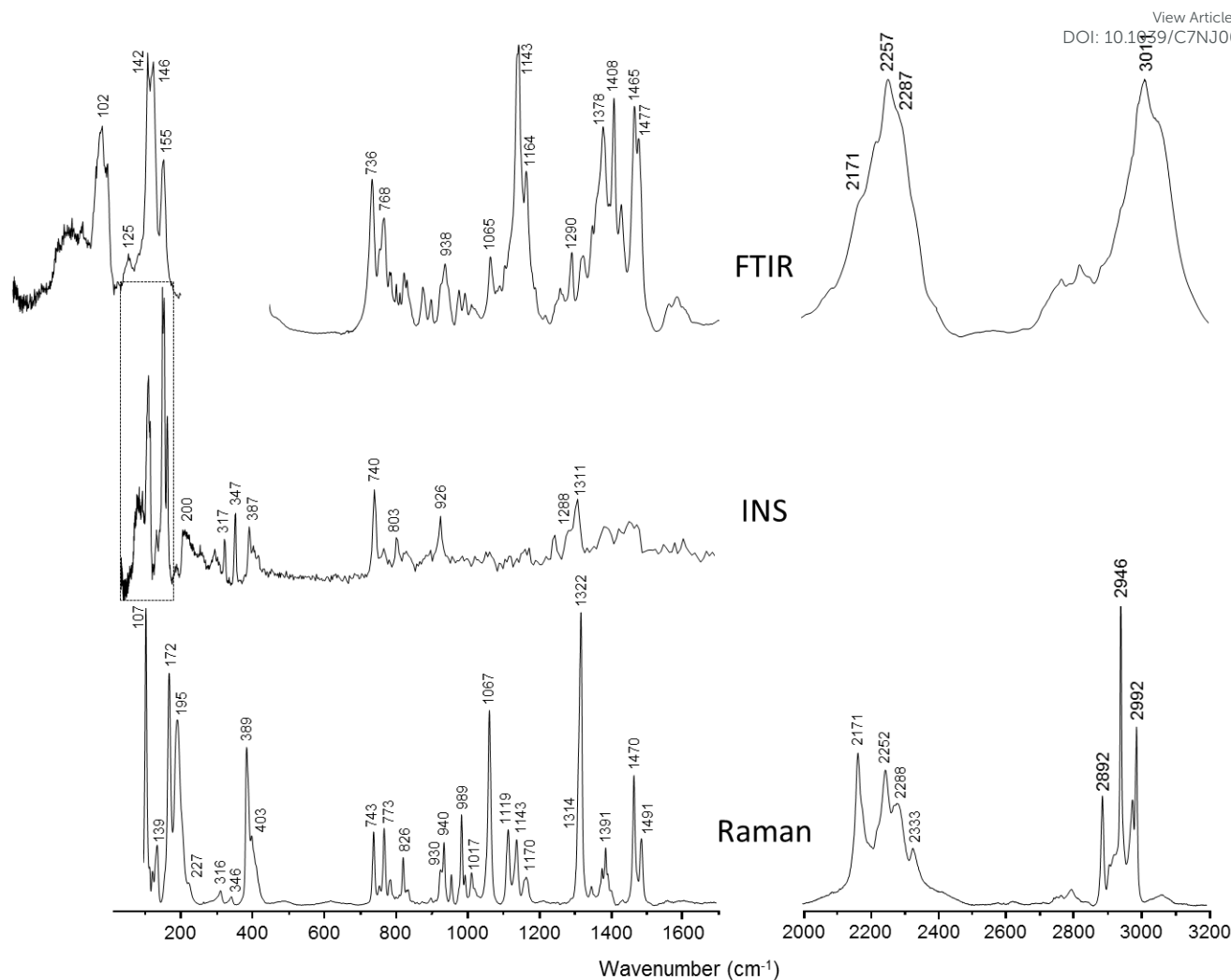


Figure 8 - FTIR (400-1700 and 2000-3200  $\text{cm}^{-1}$ ), INS (0-1700  $\text{cm}^{-1}$ ) and Raman (100-1700 and 2000-3200  $\text{cm}^{-1}$ ) spectra of solid 1,3-diaminopropane- $\text{N-d}_6^{2+}\cdot 2\text{Cl}^-$ .

In order to overcome this limitation, a methodology has recently been developed and tested to correct the vibrational frequencies predicted for the isolated amine, in its cationic form, for the effects of the interactions with the counterions, without their explicit consideration in the calculation.<sup>56</sup> The correction factors to be used were determined by considering the whole series of  $\alpha,\omega$ -diamine hydrochlorides ( $[\text{H}_3\text{N}(\text{CH}_2)_n\text{NH}_3]^{2+}\cdot 2\text{Cl}^-$ ,  $n=2-10$  and 12; for more details see<sup>56</sup>). Table 5 contains the experimental vibrational frequencies (FTIR, Raman and INS) and corresponding assignments for solid  $[\text{H}_3\text{N}(\text{CH}_2)_3\text{NH}_3]^{2+}\cdot 2\text{Cl}^-$ . The theoretically predicted frequency values before and after correction for the effects of the intermolecular interaction, anharmonicity and incomplete electron correlation treatment, are also listed for comparison. Note that the longitudinal and transversal skeletal modes (LAM and TAM) are not regarded in the methodology as they constitute a special group of vibrations.<sup>56</sup>

On the whole, it is found that correction for both intermolecular effects, by using the group correction factors previously defined,<sup>56</sup> and for anharmonicity and incomplete electron correlation treatment, using the scaling factor of 0.9499 as

suggested by Merrick *et al.*,<sup>51</sup> clearly improves the matching between observed and predicted vibrational frequencies. This is particularly obvious for the  $\nu\text{NH}_3$  and  $\tau\text{NH}_3$  modes, as they are the more prone to be affected by  $\text{N-H}\cdots\text{Cl}$  interactions, as mentioned above.

The  $\nu\text{NH}_3$  modes, predicted around  $3500\text{ cm}^{-1}$  for the isolated cation are downward shifted to about  $2900-2800\text{ cm}^{-1}$ . In other words, those modes are shifted to the spectral interval comprising the spectral features due to the  $\text{CH}_2$  stretching modes ( $\nu\text{CH}_2$ ). This is confirmed by the experimental data measured for the deuterated cationic molecule, namely by the disappearance of the bands observed between  $2900$  and  $2774\text{ cm}^{-1}$  (Figures 7 and 8; Table 5). Finally, calculations on the isolated  $[\text{H}_3\text{N}(\text{CH}_2)_2\text{NH}_3]^{2+}$  cation predict the  $\tau\text{NH}_3$  modes to occur at  $235$  and  $238\text{ cm}^{-1}$ , far below the frequency of the spectral features observed to disappear upon deuteration –  $413$  and  $447\text{ cm}^{-1}$  (Figures 7 and 8). The disappearance of these two spectral features is accompanied by the detection of new bands around  $317$  and  $347\text{ cm}^{-1}$  (Figure 8). Yet, correction of the  $235$  and  $238\text{ cm}^{-1}$  calculated values yields the wavenumbers  $549$  and  $556\text{ cm}^{-1}$ , much closer to the experimental values pointed out by the deuteration studies ( $413$  and  $447\text{ cm}^{-1}$ ).

Table 5 -Vibrational (FTIR, Raman and INS) experimental and DFT-calculated harmonic wavenumbers (cm<sup>-1</sup>) for H<sub>3</sub>N(CH<sub>2</sub>)<sub>3</sub>NH<sub>3</sub><sup>2+</sup>·2Cl<sup>-</sup> and its N-deuterated derivative in the solid state. [View Article Online](#)  
DOI: 10.1039/C7NJ00810D

| H <sub>3</sub> N(CH <sub>2</sub> ) <sub>3</sub> NH <sub>3</sub> <sup>2+</sup> |       |                    |      |      | D <sub>3</sub> N(CH <sub>2</sub> ) <sub>3</sub> ND <sub>3</sub> <sup>2+</sup> |       |                    |      |      | Sym            | Tentative assignment <sup>b</sup>  |
|---|-------|--------------------|------|------|---|-------|--------------------|------|------|----------------|--|
| Exp.  |       | Calc. <sup>a</sup> |      |      | Exp.  |       | Calc. <sup>a</sup> |      |      |                |  |
| FTIR  | Raman | INS                | (1)  | (2)  | FTIR  | Raman | INS                | (1)  | (2)  |                |  |
| -   | 53    |                    | -    | -    | -   |       |                    | -    | -    |                | External mode  |
| -   | 61    | 64                 | -    | -    | -   |       |                    | -    | -    |                | External mode  |
| -   | 71    |                    | -    | -    | -   |       |                    | -    | -    |                | External mode  |
| -   |       | 80                 | -    | -    | -   |       |                    | -    | -    |                | External mode  |
| -   | 87    | 86                 | -    | -    | -   |       | 85                 | -    | -    |                | External mode  |
| -   |       | 103                | -    | -    | -   |       | 102                | -    | -    |                |  |
| -   | 107   | 108                | -    | -    | -   | 107   | 107                | -    | -    |                | External mode  |
| -   | 126   | 127                | -    | -    | -   | 126   | 125                | -    | -    |                | External mode  |
| -   | 138   | 135                | -    | -    | -   | 139   |                    | -    | -    |                | External mode  |
| -   |       | 143                | -    | -    | -   |       | 142                | -    | -    |                |  |
| -   |       | 147                | -    | -    | -   |       | 146                | -    | -    |                | External mode  |
| -   |       | 157                | 105  | (c)  | -   |       | 155                | 92   | (c)  | A <sub>2</sub> | δ NCCN (TAM2)  |
| -   | 177   | 188                | 122  | (c)  | -   | 172   | 181                | 113  | (c)  | B <sub>1</sub> | δ NCCN (TAM1)  |
| -   | 209   | 217                | 188  | (c)  | -   | 195   | 200                | 171  | (c)  | A <sub>1</sub> | δ NCCN (LAM3)  |
| -   | 244   | 244                | -    | -    | -   | 227   |                    | -    | -    |                | (108+147 cm <sup>-1</sup> )  |
| -   |       | 291                | -    | -    | -   |       | 290                | -    | -    |                | (143+157 cm <sup>-1</sup> )  |
| -   | 408   | 407                | 386  | (c)  | -   | 389   | 387                | 363  | (c)  | A <sub>2</sub> | δ NCCN (LAM1)  |
| 427   | 428   | 426                | 417  | (c)  | -   | 403   | 399                | 381  | (c)  | B <sub>2</sub> | δ NCCN (LAM2)  |
| 447   | 445   | 447                | 235  | 549  | -   | 316   | 317                | 182  | 425  | B <sub>1</sub> | τNH <sub>3</sub> (τND <sub>3</sub> )                                       |
|   |       |                    | 238  | 556  | -   | 346   | 347                | 186  | 435  | A <sub>2</sub> | τNH <sub>3</sub> (τND <sub>3</sub> )                                       |
| 762   | 767   | 766                | 772  | 777  |   |       |                    | 731  | 736  | B <sub>1</sub> | ρNH <sub>3</sub> (ρND <sub>3</sub> ) + ρCH <sub>2</sub>                    |
| 782   |       |                    |      |      | 736   | 743   | 740                |      |      |                |  |
|   | 834   | 832                | 836  | 842  |   |       |                    | 723  | 728  | A <sub>2</sub> | ρNH <sub>3</sub> (ρND <sub>3</sub> ) + ρCH <sub>2</sub>                    |
| 939   | 933   | 937                | 926  | 932  | 768   | 773   | 766                | 760  | 765  | A <sub>1</sub> | ρNH <sub>3</sub> (ρND <sub>3</sub> )                                       |
| 945   | 944   |                    |      |      |   |       |                    |      |      |                |  |
| 960   | 961   | 959                | 951  | 958  | 786   | 789   | 803                | 802  | 808  | B <sub>1</sub> | ρNH <sub>3</sub> (ρND <sub>3</sub> ) + tCH <sub>2</sub> + ρCH <sub>2</sub> |
| 1030  |       |                    |      |      | 825   | 826   |                    |      |      |                |  |
| 1037  | 1040  | 1038               | 1030 | 1037 | 832   | 835   | 828                | 818  | 824  | B <sub>2</sub> | ρNH <sub>3</sub> (ρND <sub>3</sub> )                                       |
|   |       |                    |      |      | 927   | 930   |                    |      |      |                |  |
|   |       |                    |      |      | 938   | 940   | 926                | 943  | 950  | A <sub>2</sub> | ρND <sub>3</sub> + ρCH <sub>2</sub> + tCH <sub>2</sub>                     |
|   |       |                    |      |      | 960   |       |                    |      |      |                |  |
|   |       |                    |      |      | 978   | 989   |                    | 1075 | 991  | B <sub>2</sub> | ν <sub>s</sub> CC  |
|   |       |                    |      |      | 994   | 998   |                    |      |      |                |  |
| 1021  |       |                    | 921  | 1024 | 1012  | 1017  |                    | 912  | 1014 | B <sub>2</sub> | ν <sub>a</sub> NC  |
| 1103  |       | 1103               | 1116 | 1124 |   |       |                    |      |      | B <sub>2</sub> | ρNH <sub>3</sub> + ν <sub>a</sub> CC                                       |
|   | 1103  |                    | 1016 | 1129 | 1065  | 1067  |                    | 970  | 1078 | A <sub>1</sub> | ν <sub>s</sub> NC  |
| 1189  | 1190  | 1188               | 1243 | 1181 |   | 1119  |                    | 1197 | 1137 | B <sub>1</sub> | ρCH <sub>2</sub> + ρNH <sub>3</sub> (ρND <sub>3</sub> )                    |
| 1216  |       | 1224               | 1204 | 1212 | 1143  | 1143  |                    | 1132 | 1140 | A <sub>1</sub> | ρNH <sub>3</sub> (ρND <sub>3</sub> ) + ν <sub>s</sub> CC                   |
|   | 1304  |                    | 1355 | 1287 |   |       | 1247               | 1317 | 1251 | A <sub>2</sub> | tCH <sub>2</sub>   |
| 1310  |       | 1311               | 1373 | 1304 | 1291  |       | 1288               | 1358 | 1290 | B <sub>2</sub> | ωCH <sub>2</sub>   |
|   | 1325  | 1326               | 1390 | 1320 |   | 1322  |                    | 1386 | 1317 | A <sub>2</sub> | tCH <sub>2</sub>   |
| 1335  | 1339  |                    | 1405 | 1335 | 1321  | 1314  | 1311               | 1384 | 1315 | B <sub>1</sub> | tCH <sub>2</sub>   |
|   | 1395  |                    | 1462 | 1389 | 1378  | 1381  | 1392               | 1454 | 1381 | A <sub>1</sub> | ωCH <sub>2</sub>   |
| 1409  |       | 1404               | 1476 | 1402 | 1408  | 1391  |                    | 1476 | 1402 | B <sub>2</sub> | ωCH <sub>2</sub>   |
| 1457  | 1462  |                    | 1523 | 1447 | 1465  | 1470  | 1460               | 1523 | 1447 | A <sub>1</sub> | αCH <sub>2</sub>   |
| 1464  | 1472  | 1472               |      |      |   |       |                    |      |      |                |  |
| 1479  | 1486  |                    | 1537 | 1460 | 1477  | 1491  | 1479               | 1537 | 1460 | A <sub>1</sub> | αCH <sub>2</sub>   |
|   |       |                    | 1589 | 1524 |   |       |                    | 1220 | 1170 | B <sub>2</sub> | δ <sub>s</sub> NH <sub>3</sub> (δ <sub>s</sub> ND <sub>3</sub> )           |
|   |       |                    | 1591 | 1526 |   |       |                    | 1223 | 1173 | A <sub>1</sub> | δ <sub>s</sub> NH <sub>3</sub> (δ <sub>s</sub> ND <sub>3</sub> )           |
|   |       |                    | 1704 | 1635 |   |       |                    | 1228 | 1178 | B <sub>2</sub> | δ <sub>as</sub> NH <sub>3</sub> (δ <sub>as</sub> ND <sub>3</sub> )         |
| 1600  | 1604  | 1613               | 1706 | 1637 | 1164  | 1170  | 1164               | 1229 | 1179 | A <sub>1</sub> | δ <sub>as</sub> NH <sub>3</sub> (δ <sub>as</sub> ND <sub>3</sub> )         |
|   |       |                    | 1711 | 1642 |   |       |                    | 1230 | 1180 | A <sub>2</sub> | δ <sub>as</sub> NH <sub>3</sub> (δ <sub>as</sub> ND <sub>3</sub> )         |
|   |       |                    | 1711 | 1642 |   |       |                    | 1231 | 1181 | B <sub>1</sub> | δ <sub>as</sub> NH <sub>3</sub> (δ <sub>as</sub> ND <sub>3</sub> )         |

|      |      |      |      |      |      |      |      |                |  |   |
|------|------|------|------|------|------|------|------|----------------|--|---|
| 2895 |      | 3406 | 2847 | 2171 |      | 2443 | 2042 | B <sub>2</sub> | v <sub>s</sub> NH <sub>3</sub> (v <sub>s</sub> ND <sub>3</sub> )   | View Article Online<br>10.1039/C7NJ00810D |
|      | 2900 | 3408 | 2849 |      | 2171 | 2445 | 2044 | A <sub>1</sub> | v <sub>s</sub> NH <sub>3</sub> (v <sub>s</sub> ND <sub>3</sub> )   |   |
|      |      | 3490 | 2917 |      |      | 2574 | 2152 | B <sub>2</sub> | v <sub>as</sub> NH <sub>3</sub> (v <sub>as</sub> ND <sub>3</sub> ) |   |
|      | 3030 | 3491 | 2918 | 2257 | 2252 | 2575 | 2152 | A <sub>1</sub> | v <sub>as</sub> NH <sub>3</sub> (v <sub>as</sub> ND <sub>3</sub> ) |   |
|      |      | 3502 | 2927 |      |      | 2585 | 2161 | A <sub>2</sub> | v <sub>as</sub> NH <sub>3</sub> (v <sub>as</sub> ND <sub>3</sub> ) |   |
| 3059 | 3053 | 3503 | 2928 | 2287 | 2288 | 2585 | 2161 | B <sub>1</sub> | v <sub>as</sub> NH <sub>3</sub> (v <sub>as</sub> ND <sub>3</sub> ) |   |
|      |      | 3077 | 2923 | 2896 | 2892 | 3077 | 2923 | A <sub>1</sub> | v <sub>s</sub> C <sup>7</sup> H <sub>2</sub>                       |   |
|      | 2889 | 3129 | 2972 |      | 2946 | 3129 | 2972 | B <sub>1</sub> | v <sub>as</sub> C <sup>7</sup> H <sub>2</sub>                      |   |
|      | 2943 | 3134 | 2977 |      | 2980 | 3134 | 2977 | B <sub>2</sub> | v <sub>s</sub> CH <sub>2</sub>                                     |   |
|      | 2976 | 3137 | 2980 |      | 2992 | 3137 | 2980 | A <sub>1</sub> | v <sub>s</sub> CH <sub>2</sub>                                     |   |
|      | 2989 | 3201 | 3041 | 3011 |      | 3201 | 3041 | B <sub>1</sub> | v <sub>as</sub> CH <sub>2</sub>                                    |   |
| 3010 |      | 3197 | 3037 |      |      | 3197 | 3037 | A <sub>2</sub> | v <sub>as</sub> CH <sub>2</sub>                                    |   |

<sup>a</sup> column (1) - uncorrected and unscaled mPW1PW/6-31G\* calculated frequencies for isolated H<sub>3</sub>N(CH<sub>2</sub>)<sub>3</sub>NH<sub>3</sub><sup>2+</sup> (TT conformer; C<sub>2v</sub> symmetry); column (2) - corrected (using the group correction factors reported in [52]) and scaled (using a scaling factor of 0.9499 as suggested by Merrick et al. [50]) mPW1PW/6-31G\* calculated frequencies for isolated H<sub>3</sub>N(CH<sub>2</sub>)<sub>3</sub>NH<sub>3</sub><sup>2+</sup> (TT conformer; C<sub>2v</sub> symmetry). <sup>b</sup> δ, deformation; τ, torsion; ω, wagging; t, twisting; ρ - rocking; α, scissoring; v, stretching; s, symmetric; a, antisymmetric; TAM, Transverse Acoustic Mode; LAM, Longitudinal Acoustic Mode. <sup>c</sup> not calculated with this method, see text.

## Conclusions

In the present work, a conformational analysis of one of the smallest alkyl polyamines, 1,3-diaminopropane, was performed by several complementary vibrational techniques, both optical – FTIR and Raman – and inelastic neutron scattering, coupled to DFT calculations.

These calculations, using the mPW1PW functional and the 6-31G\* basis set, were carried out for four distinct systems: isolated molecule and condensed phase, and solutions in water and carbon tetrachloride (at the SCRF-PCM level). For each environment, more than two dozen real minima in the potential energy surface were found. The most stable conformers, both in the gaseous phase and in CCl<sub>4</sub> solution, were GGG'G and TG'GG'. For both the liquid phase and the aqueous solution, in turn, TTTT, TGTT and TTTG were the predominant species.

Vibrational spectra were measured for the pure compound (liquid and solid phases), carbon tetrachloride and aqueous solutions (at different molar fractions), as well as for the N-ionised and N-deuterated species. Assignments of the vibrational patterns were carried out in the light of the corresponding calculated harmonic vibrational frequencies, isotopic substitution (N-deuteration) and by comparison with similar molecules previously studied by the authors (e.g. 1,2-diaminoethane<sup>9</sup>).

The experimental spectra corroborate the assessment that has been done by the theoretical calculations: i) liquid 1,3-diaminopropane (either pure or in solution) consists of a simultaneous equilibria of different conformers, some of them with skeletal gauche arrangements; ii) in the solid samples (both 1,3-diaminopropane and its N-protonated counterpart) only the *all-trans* conformers are present; iii) the conformational equilibria in aqueous solution is similar to the one of pure liquid however, a hydrophobic repulsive interaction between the water molecules and the methylene groups of 1,3-dap leading to an additional stabilisation of the conformers with a *gauche* arrangement of the alkyl chain and a slightly lower conformational dispersion.

This type of conformational studies on compounds with putative pharmacological interest is of the utmost relevance for

understanding their structure-activity relationships aiming at future applications in the field of biomedicine. In the particular case of 1,3-diaminopropane, the results presently obtained allow it to be considered as very suitable ligand for Pt(II) and Pd(II) coordination, yielding complexes (either mono- or dinuclear) with a potential antitumour ability (through DNA-binding), attending to the conformational characteristics currently unveiled. This will greatly contribute for a rational design of improved metal-based anticancer agents, displaying higher efficacy coupled to lower toxicity and acquired resistance.

## Acknowledgements

The authors thank financial support from the Portuguese Foundation for Science and Technology – UID/Multi/00070/2013 and PTDC/QEQ-MED/1890/2014 (within Project 3599 – Promote Scientific Production and Technological Development as well as the Formation of Thematic Networks (3599-PPCDT) – jointly financed by the European Community Fund FEDER). The STFC Rutherford Appleton Laboratory is thanked for access to neutron beam facilities. Acknowledgements are also due to Laboratório Associado CICECO, University of Aveiro, Portugal, for the access to computational facilities (Gaussian 09 program).

## Notes and references

- J.J.C. Teixeira-Dias, L.A.E. Batista de Carvalho, A.M. Amorim da Costa, I.M.S. Lampreia and E.F.G. Barbosa, *Spectrochim. Acta*, 1986, **42A**, 589.
- N. Sato, Y. Hamada and M. Tsuboi, *Spectrochim. Acta*, 1987, **43A**, 943.
- L.A.E. Batista de Carvalho, A.M. Amorim da Costa, M.L. Duarte and J.J.C. Teixeira-Dias, *Spectrochim. Acta*, 1988, **44A**, 723.
- J.R. Durig, W.B. Beshir, S.E. Godbey and T.J. Hizer, *J. Raman Spectrosc.*, 1989, **20**, 311.
- L.A.E. Batista de Carvalho, A.M. Amorim da Costa and J.J.C. Teixeira-Dias, *J. Molec. Struct.-Theochem*, 1990, **64**, 327.
- L.A.E. Batista de Carvalho, J.J.C. Teixeira-Dias and R. Fausto, *Struct. Chem.*, 1990, **1**, 533.
- L.R. Schmitz and N.L. Allinger, *J. Am. Chem. Soc.*, 1990, **112**, 8307.



- 8 L.A.E. Batista de Carvalho and J.J.C Teixeira-Dias, *J. Raman Spectrosc.*, 1995, **26**, 653.
- 9 L.A.E. Batista de Carvalho, L.E. Lourenço and M.P.M. Marques, *J.Molec.Struct.* 1999, **482**, 639.
- 10 M.P.M. Marques and L.A.E. Batista de Carvalho, in *COST 917: Biogenically Active Amines in Food, Vol. IV*, Eds D. M. L. Morgan, A. White, F. Sanchez-Jimenez, S. Bardocz, Book Series: European Commission – Science Research Development, 2000, 122-129.
- 11 A.M. Amorim da Costa, M.P.M. Marques and L.A.E. Batista de Carvalho, *J.Raman Spec.*, 2003, **34**, 357.
- 12 J.R. Durig, C. Zheng, T.K. Gounev, W.A. Herrebout and B.J. van der Veken, *J.Phys.Chem. A*, 2006, **110**, 5674.
- 13 O. Alver and C. Parlak, *J. Theor. Comput. Chem.*, 2010, **9**, 667.
- 14 S. Padrão, S.M. Fiuza, A.M. Amado, A.M. Amorim da Costa and L.A.E. Batista de Carvalho, *J Phys. Org. Chem*, 2011, **24**, 110.
- 15 M. Tursun, G. Kesan, C. Parlak and M. Senyel, *Spectrochim. Acta*, 2013, **114A**, 668.
- 16 T.M. Silva, S.M. Fiuza, M.P.M. Marques, L.A.E. Batista de Carvalho and A.M. Amado, *Spectrochim.Acta*, 2016, **157A**, 227.
- 17 M. Caceres, A. Lobato, N.J. Mendoza, L.J. Bonales and V.G. Baonza, *PCCP*, 2016, **18**, 26192.
- 18 A.M. Amorim da Costa, M.P.M. Marques and L.A.E. Batista de Carvalho, *Vib.Spectrosc.*, 2004, **35**, 165.
- 19 H.M. Wallace, A.V. Fraser and A. Hughes, *Biochem. J.*, 2003, **376**, 1.
- 20 J.E. Seely and A.E. Pegg, *Biochem. J.*, 1983, **216**, 701.
- 21 E.I. Salim, H. Wanibuchi, K. Morimura, S. Kim, Y. Yano, S. Yamamoto and S. Fukushima, *Carcinogenesis*, 2000, **21**, 195.
- 22 E.W. Gerner and F.L. Meyskens, *Nature Reviews Cancer*, 2004, **4**, 781.
- 23 S.L. Nowotarski, P.M. Woster and R.A. Casero, Jr., *Expert Rev Mol Med.*, 2013, **15**, e3.
- 24 M.P.M. Marques, L.A.E. Batista de Carvalho and J. Tomkinson, *J.Phys.Chem. A*, 2002, **106**, 2473.
- 25 L.A.E. Batista de Carvalho, M.P.M. Marques and J. Tomkinson, *J.Phys.Chem. A*, 2006, **110**, 12947.
- 26 V.L. Gein, V.V. Yushkov Y, N. N. Kasimova, M. A. Panina, N. S. Rakshina, L. V. Strelkova and E. V. Voronina, *Pharm. Chem. J.*, 2007, **41**, 367.
- 27 C.G. Van Kralingen, J. Reedijk and A. L. Spek, *Inorganic Chemistry*, 1980, **19**, 1481.
- 28 A. Alvarez-Valdés, J.M. Pérez, I. López-Solera, R. Lannegrand, J.M. Contiente, P. Amo-Ochoa, M.J. Camazón, X. Solans, M. Font-Bardía and C. Navarro-Ranninger, *J. Med. Chem.*, 2002, **45**, 1835.
- 29 H. Silva, C.V. Barra, C. França da Costa, M. Vieira de Almeida, E.T. César, J.N. Silveira, A. Garnier-Suillerot, F.C. Silva de Paula, E.C. Pereira-Maia, and A.P.S. Fontes, *J. Inorg. Biochem.*, 2008, **102**, 767.
- 30 A.L.M. Batista de Carvalho, S.M. Fiuza, J. Tomkinson, L.A.E. Batista de Carvalho and M.P.M. Marques, *Spectrosc.-Int. J.*, 2012, **27**, 403.
- 31 J. Ferlay, I. Soerjomataram, R. Dikshit, S. Eser, C. Mathers, M. Rebelo, D. M. Parkin, D. Forman and F. Bray, *Int. J. Cancer*, 2015, **136**, E359.
- 32 L. Kelland, *Nat. Rev. Cancer*, 2007, **7**, 573.
- 33 N.P. Farrell, *Curr. Top. Med. Chem.*, 2011, **11**, 2623.
- 34 Y. Li, Y. Li, J. Li, G. Pi and W. Tan, *Oncotargets Ther.*, 2014, **7**, 1361.
- 35 M.T. Truong, J. Winzelberg and K.W.Chang, *Int. J. Pediatr. Otorhi.*, 2007, **71**, 1631.
- 36 X. Yao, K. Panichpisal, N. Kurtzman and K.Nugent, *Am. J. Med. Sci.*, 2007, **334**, 115.
- 37 S.M.Fiuza, A.M. Amado, Paulo J. Oliveira, Vilma A. Sardão, L.A.E. Batista de Carvalho and M.P.M. Marques, *Lett. Drug Des. Discov.*, 2006, **3**, 149.
- 38 A.S. Soares, S.M. Fiuza, M.J. Gonçalves, L.A.E. Batista de Carvalho, M.P.M. Marques and A.M. Urbano, *Lett. Drug Des. Discov.*, 2007, **4**, 460.
- 39 C. Mitchell, P. Kabolizadeh, J. Ryan, J.D. Roberts, A. Yacoub, D.T. Curiel, P.B. Fisher, M.P. Hagan, N.P. Farrell, S. Grant and P. Dent, *Molec.Pharmac.*, 2007, **72**, 704.
- 40 A. Hegmans, J. Kasparkova, O. Vrana, L.R. Kelland, V. Brabec and N.P Farrell, *J.Med.Chem.*, 2008, **51**, 2254.
- 41 R. Tummala, P. Diegelman, S.M. Fiuza, L.A.E. Batista de Carvalho, M.P.M. Marques, D.L. Kramer, K. Clark, S. Vulcic, C.W. Porter and L. Pendyala, *Oncol. Rep.*, 2010, **24**, 15.
- 42 S. M. Fiuza, J. Holy, L.A.E. Batista de Carvalho and M.P.M. Marques, *Chem. Biol. Drug Des.*, 2011, **77**, 477.
- 43 S.M. Fiuza, A.M. Amado, S.F. Parker, M.P.M. Marques and L.A.E. Batista de Carvalho, *New J. Chem*, 2015, **39**, 6274.
- 44 A.L.M. Batista de Carvalho, M. Pilling, P. Gardner, J. Doherty, G. Cinque, K. Wehbe, C. Kelley, L.A.E. Batista de Carvalho and M.P.M. Marques, *Faraday Discuss.*, 2016, **187**, 273.
- 45 S.F. Parker, F. Fernandez-Alonso, A.J. Ramirez-Cuesta, J. Tomkinson, S. Rudic, R.S. Pinna, G. Gorini and J. Fernández Castañón, *J. Phys. Conf. Series*, 2014, **554**, 012003.
- 46 ISIS - STFC - TOSCA, <http://www.isis.stfc.ac.uk/instruments/tosca/>, 2017 (accessed 01.03.17).
- 47 Gaussian 09, Revision A.02, M. J. Frisch, G. W. Trucks, H. B. Schlegel, G. E. Scuseria, M. A. Robb, J. R. Cheeseman, G. Scalmani, V. Barone, G. A. Petersson, H. Nakatsuji, M. Caricato, X. Li, A. Marenich, J. Bloino, B. G. Janesko, R. Gomperts, B. Mennucci, H. P. Hratchian, J. V. Ortiz, A. F. Izmaylov, J. L. Sonnenberg, D. Williams-Young, F. Ding, F. Lipparini, F. Egidi, J. Goings, B. Peng, A. Petrone, T. Henderson, D. Ranasinghe, V. G. Zakrzewski, J. Gao, N. Rega, G. Zheng, W. Liang, M. Hada, M. Ehara, K. Toyota, R. Fukuda, J. Hasegawa, M. Ishida, T. Nakajima, Y. Honda, O. Kitao, H. Nakai, T. Vreven, K. Throssell, J. A. Montgomery, Jr., J. E. Peralta, F. Ogliaro, M. Bearpark, J. J. Heyd, E. Brothers, K. N. Kudin, V. N. Staroverov, T. Keith, R. Kobayashi, J. Normand, K. Raghavachari, A. Rendell, J. C. Burant, S. S. Iyengar, J. Tomasi, M. Cossi, J. M. Millam, M. Klene, C. Adamo, R. Cammi, J. W. Ochterski, R. L. Martin, K. Morokuma, O. Farkas, J. B. Foresman, and D.J. Fox, Gaussian, Inc., Wallingford CT, 2016.
- 48 C. Adamo and V. Barone, *J. Chem. Phys.* 1998, **108**, 699.
- 49 J.P. Perdew, K. Burke and Y. Wang, *Phys. Rev. B*, 1996, **54**, 16533.
- 50 P.C. Hariharan and J.A. Pople, *Theor. Chim. Acta*, 1973, **28**, 213.
- 51 J.P. Merrick, D. Moran and L. Radom, *J. Phys. Chem. A*, 2007, **111**, 11683.
- 52 J.-D. Chai and M. Head-Gordon, *Phys. Chem. Chem. Phys.*, 2008, **10**, 6615.
- 53 Y. Zhao and D. G. Truhlar, *Theor. Chem. Acc.*, 2008, **120**, 215.
- 54 G. D. Purvis III and R. J. Bartlett, *J. Chem. Phys.*, 1982, **76**, 1910.
- 55 A.M. Amado, J.C. Otero, M.P.M. Marques and L.A.E. Batista de Carvalho, *ChemPhysChem.*, 2004, **5**, 1837.
- 56 S.M. Fiuza, T.M. Silva, M.P.M. Marques, L.A.E. Batista de Carvalho and A.M. Amado, *J.Mol.Model.*, 2015, **21**, Article 26

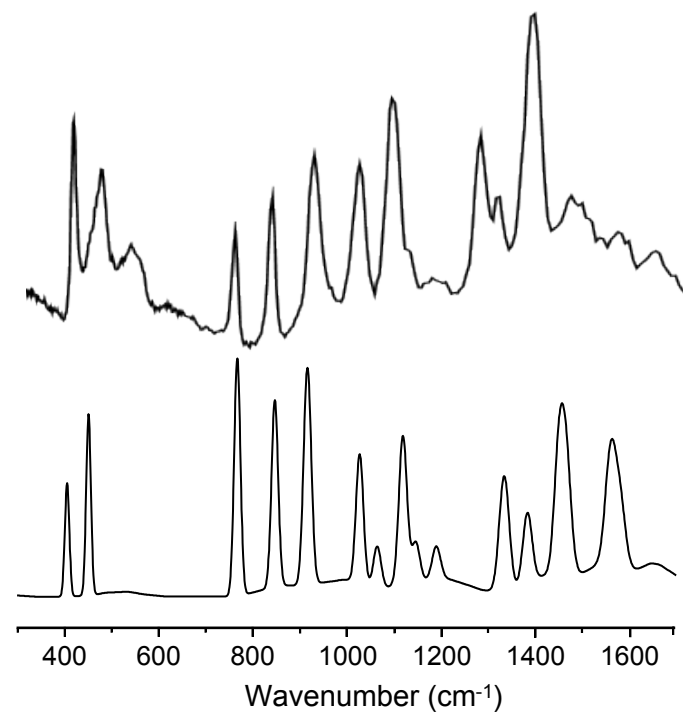


Figure S1 – Experimental INS (100-1650 cm<sup>-1</sup>) spectrum of pure 1,3-diaminopropane in the solid phase (top) and the mPW1PW/6-31G(d) calculated spectrum for the major TTTT conformer (bottom).

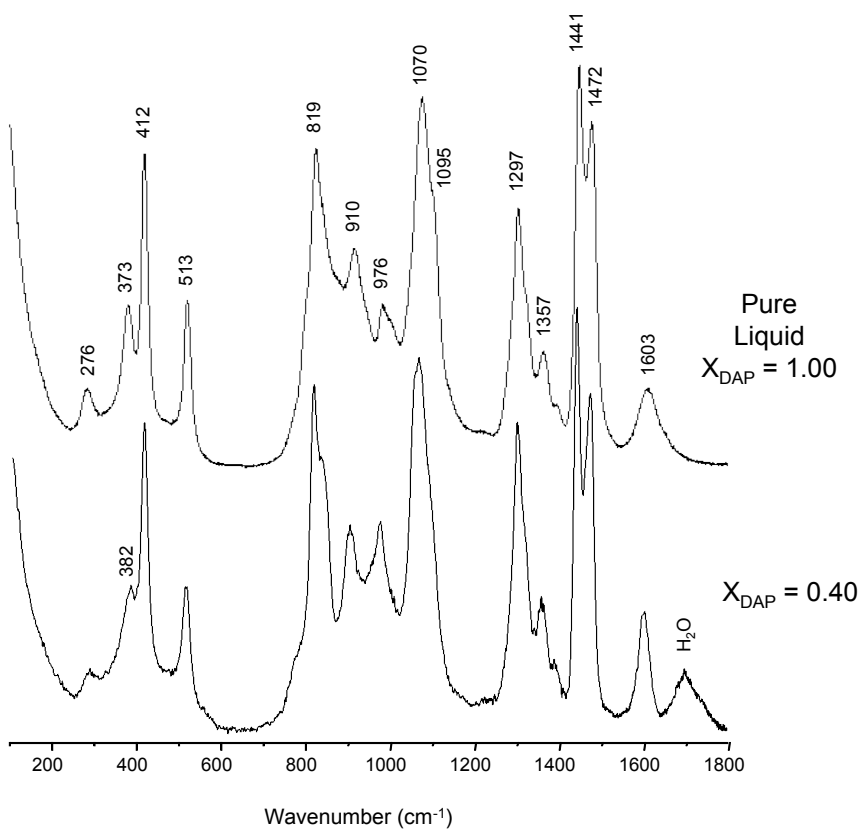


Figure S2 - Raman (100-1800 cm<sup>-1</sup>) spectra of pure 1,3-diaminopropane in the liquid phase (upper) and in water solution for an amine molar fraction 0.40 (bottom).

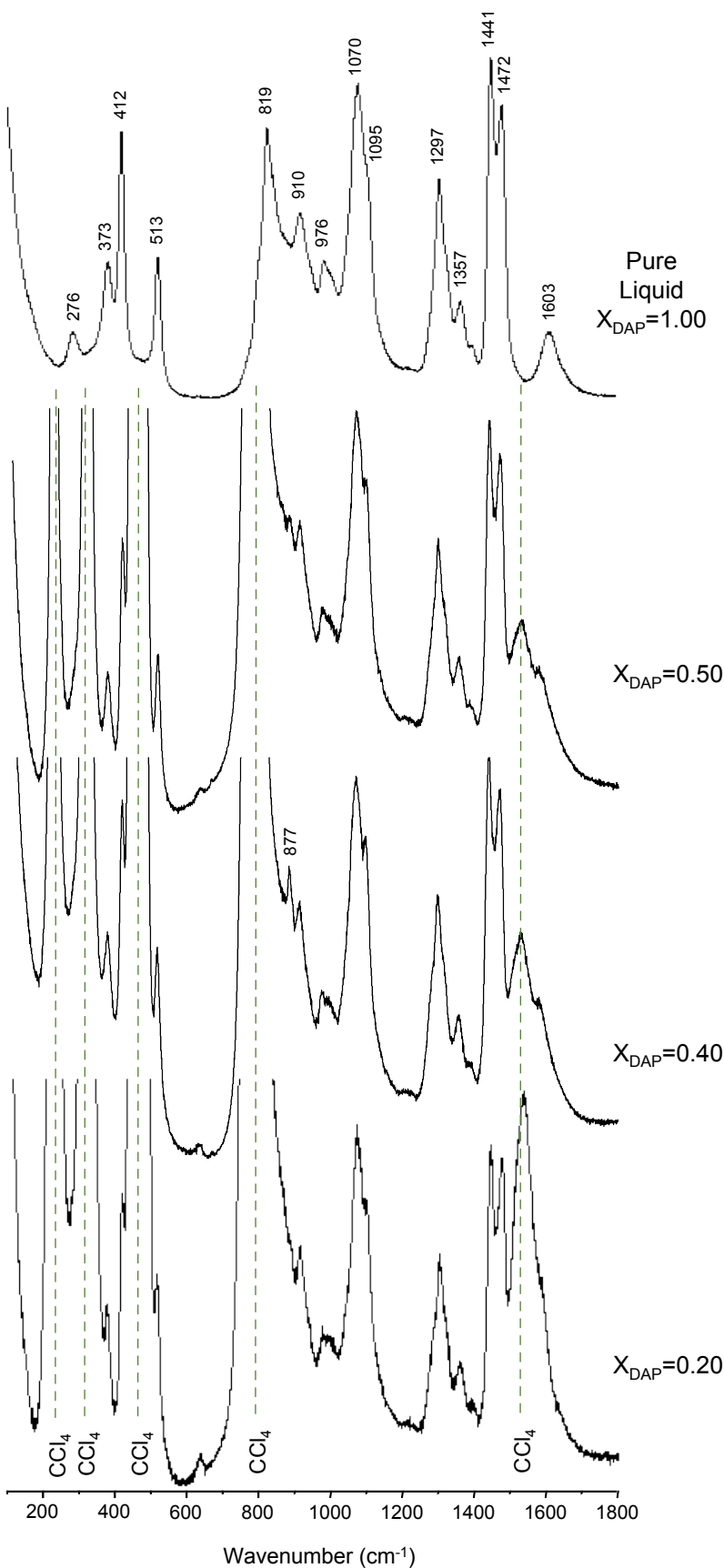


Figure S3 - Raman (100-1800 cm<sup>-1</sup>) spectra of pure 1,3-diaminopropane in the liquid phase (top) and of 1,3-diaminopropane/ $\text{CCl}_4$  solutions at different molar fractions.

**Table S1.** Calculated conformational energies, for the 1,3-dap conformers.

| Conformer <sup>a</sup> | CCSD(T)                               |                                       | mPW1PW                                |                                       | wB97XD                                |                                       | M06-2X                                |  |
|------------------------|---------------------------------------|---------------------------------------|---------------------------------------|---------------------------------------|---------------------------------------|---------------------------------------|---------------------------------------|--|
|                        | $\Delta E$<br>(kJ.mol <sup>-1</sup> ) | $\Delta E$<br>(kJ.mol <sup>-1</sup> ) | $\Delta G$<br>(kJ.mol <sup>-1</sup> ) | $\Delta E$<br>(kJ.mol <sup>-1</sup> ) | $\Delta G$<br>(kJ.mol <sup>-1</sup> ) | $\Delta E$<br>(kJ.mol <sup>-1</sup> ) | $\Delta G$<br>(kJ.mol <sup>-1</sup> ) |  |
| GGG'G                  | 0.00                                  | 0.00                                  | 0.00                                  | 0.00                                  | 0,00                                  | 0,00                                  | 0.00                                  |  |
| TG'GG'                 | 4.11                                  | 1.03                                  | 0.64                                  | 2.58                                  | 1.31                                  | 3.50                                  | 2.14                                  |  |
| TGGG'                  | 3.56                                  | 4.04                                  | 2.30                                  | 2.95                                  | 0.63                                  | 2.00                                  | 0.66                                  |  |
| TTTT                   | 6.29                                  | 5.39                                  | 3.52                                  | 6.22                                  | 3.48                                  | 7.82                                  | 6.44                                  |  |
| GGGG'                  | 1.14                                  | 4.28                                  | 3.67                                  | 2.91                                  | 1.66                                  | 0.41                                  | 0.29                                  |  |
| GG'G'G                 | 1.26                                  | 5.94                                  | 3.11                                  | 4.62                                  | 2.81                                  | 3.88                                  | 2.59                                  |  |
| TTGG'                  | 3.64                                  | 6.44                                  | 2.56                                  | 6.43                                  | 2.91                                  | 6.86                                  | 2.78                                  |  |
| TTTG                   | 5.52                                  | 6.65                                  | 2.74                                  | 6.77                                  | 2.55                                  | 7.91                                  | 2..83                                 |  |
| TGTT                   | 7.52                                  | 6.41                                  | 3.04                                  | 6.31                                  | 1.98                                  | 7.88                                  | 2.68                                  |  |
| GTGG'                  | 4.21                                  | 6.92                                  | 3.57                                  | 6.28                                  | 2.52                                  | 6.13                                  | 2.35                                  |  |
| TGTG                   | 6.40                                  | 7.25                                  | 3.84                                  | 6.45                                  | 2.24                                  | 7.36                                  | 2.93                                  |  |
| TGGT                   | 7.83                                  | 6.54                                  | 6.09                                  | 4.85                                  | 4.20                                  | 6.23                                  | 4.31                                  |  |
| RMSD <sup>b</sup>      |                                       | 2.281                                 | 2.417                                 | 1.853                                 | 2.894                                 | 1.733                                 | 2.485                                 |  |

<sup>a</sup> See Figure 1; <sup>b</sup> Root-mean-square deviation

**Table S2.** Calculated (mPW1PW/6-31G\*) conformational energies, populations ( $P_i$ ), thermochemical data (at 298.15 K and 1 atm) and dipole moments ( $\mu$ ), for the 1,3-dap conformers in aqueous solution (SCRF-PCM)

| Conformer <sup>a</sup> | $s_i$ | $\Delta E$<br>(kJmol <sup>-1</sup> ) | $\Delta E_{zpv}$ <sup>b</sup><br>(kJmol <sup>-1</sup> ) | $P_i(\Delta E_{zpv})$ <sup>c</sup><br>(%) | $\Delta H$<br>(kJmol <sup>-1</sup> ) | $T\Delta S$<br>(kJmol <sup>-1</sup> ) | $\Delta G$<br>(kJmol <sup>-1</sup> ) | $P_i(\Delta G)$ <sup>d</sup><br>(%) | $\mu$ <sup>e</sup><br>(D) |
|------------------------|-------|--------------------------------------|---|---|--------------------------------------|---------------------------------------|--------------------------------------|-------------------------------------|---------------------------|
| GGG'G                  | 2     | 4.60                                 | 6.03  | 2.5                                       | 5.05                                 | -0.75                                 | 5.80                                 | 1.5                                 | 2.53                      |
| TG'GG'                 | 2     | 2.49                                 | 4.36  | 4.9                                       | 3.32                                 | -0.94                                 | 4.26                                 | 2.9                                 | 4.03                      |
| TGGG'                  | 2     | 3.96                                 | 4.21  | 5.3                                       | 3.99                                 | 2.62                                  | 1.37                                 | 9.4                                 | 3.58                      |
| TTTT                   | 1     | 0.00                                 | 0.00  | 15.0                                      | 0.00                                 | 0.00                                  | 0.00                                 | 8.3                                 | 2.65                      |
| GGGG'                  | 2     | 6.87                                 | 7.66  | 1.3                                       | 7.23                                 | 1.29                                  | 5.93                                 | 1.4                                 | 2.10                      |
| GG'G'G                 | 2     | 6.74                                 | 6.57  | 2.0                                       | 6.32                                 | 1.25                                  | 5.06                                 | 2.0                                 | 1.60                      |
| TTGG'                  | 2     | 3.64                                 | 3.31  | 7.6                                       | 3.26                                 | 1.95                                  | 1.32                                 | 9.6                                 | 3.66                      |
| TTTG                   | 2     | 2.48                                 | 2.21  | 12.0                                      | 2.27                                 | 1.92                                  | 0.35                                 | 14.3                                | 2.20                      |
| TGTT                   | 2     | 1.99                                 | 2.18  | 12.2                                      | 2.00                                 | 1.56                                  | 0.43                                 | 13.8                                | 2.04                      |
| GTGG'                  | 2     | 5.77                                 | 5.45  | 3.2                                       | 5.37                                 | 1.74                                  | 3.63                                 | 3.7                                 | 1.88                      |
| TGTG                   | 2     | 3.94                                 | 4.02  | 5.7                                       | 3.85                                 | 1.52                                  | 2.32                                 | 6.3                                 | 2.24                      |
| TGGT                   | 2     | 2.56                                 | 4.17  | 5.3                                       | 3.40                                 | -1.44                                 | 4.84                                 | 2.2                                 | 1.32                      |
| GTTG                   | 2     | 4.85                                 | 4.44  | 4.8                                       | 4.58                                 | 0.36                                  | 4.22                                 | 2.9                                 | 1.91                      |
| GTG'G                  | 2     | 6.81                                 | 6.38  | 2.1                                       | 6.40                                 | 2.17                                  | 4.23                                 | 2.9                                 | 2.05                      |
| TTGG                   | 2     | 4.73                                 | 5.06  | 3.7                                       | 4.85                                 | 1.33                                  | 3.51                                 | 3.9                                 | 2.06                      |
| TGTG'                  | 2     | 4.71                                 | 4.65  | 4.4                                       | 4.56                                 | 1.80                                  | 2.75                                 | 5.3                                 | 2.65                      |
| GTTG'                  | 1     | 5.23                                 | 4.73  | 2.1                                       | 4.91                                 | 2.21                                  | 2.69                                 | 2.7                                 | 3.54                      |
| TGGG                   | 2     | 6.23                                 | 6.28  | 2.2                                       | 6.06                                 | 1.69                                  | 4.37                                 | 2.7                                 | 2.56                      |
| GTG'G'                 | 2     | 7.47                                 | 7.46  | 1.4                                       | 7.39                                 | 1.71                                  | 5.67                                 | 1.6                                 | 2.19                      |
| GGTG                   | 2     | 6.91                                 | 6.95  | 1.7                                       | 6.81                                 | 1.53                                  | 5.28                                 | 1.9                                 | 3.49                      |
| GGGG                   | 2     | 9.06                                 | 9.90  | 0.5                                       | 9.51                                 | -0.51                                 | 10.02                                | 0.3                                 | 2.42                      |
| TGGT                   | 1     | 11.36                                | 11.39   | 0.1                                       | 11.43                                | 3.67                                  | 7.76                                 | 0.3                                 | 1.39                      |
| GGG'G'                 | 1     | 13.23                                | 14.38   | 0.0                                       | 13.80                                | 0.13                                  | 13.67                                | 0.0                                 | 3.62                      |

<sup>a</sup> See Figure 1; <sup>b</sup>  $\Delta E_{zpv}$ , zero-point vibrational energy corrected relative energies; <sup>c</sup> population according to  $\Delta E_{zpv}$  values; <sup>d</sup> population according to  $\Delta G$  values; <sup>e</sup> 1 D =  $1/3 \times 10^{-29}$  C m

**Table S3.** Calculated (mPW1PW/6-31G\*) conformational energies, populations ( $P_i$ ), thermochemical data (at 298.15 K and 1 atm) and dipole moments ( $\mu$ ), for the 1,3-dap conformers in carbon tetrachloride solution (SCRF-PCM)

| Conformer <sup>a</sup> | $s_i$ | $\Delta E$<br>(kJ.mol <sup>-1</sup> ) | $\Delta E_{zpvE}$ <sup>b</sup><br>(kJ.mol <sup>-1</sup> ) | $P_i(\Delta E_{zpvE})$ <sup>c</sup><br>(%) | $\Delta H$<br>(kJ.mol <sup>-1</sup> ) | $T\Delta S$<br>(kJ.mol <sup>-1</sup> ) | $\Delta G$<br>(kJ.mol <sup>-1</sup> ) | $P_i(\Delta G)$ <sup>d</sup><br>(%) | $\mu$ <sup>e</sup><br>(D) |
|------------------------|-------|---------------------------------------|---|--|---------------------------------------|--|---------------------------------------|-------------------------------------|---------------------------|
| GGG'G                  | 2     | 0.18                                  | 0.13  | 13.8                                       | 0.07                                  | -0.37                                  | 0.44                                  | 8.8                                 | 2.09                      |
| TG'GG'                 | 2     | 0.00                                  | 0.00  | 14.6                                       | 0.00                                  | -0.20                                  | 0.20                                  | 9.7                                 | 3.54                      |
| TGGG'                  | 2     | 2.71                                  | 1.94  | 6.5  | 2.43                                  | 2.00                                   | 0.43                                  | 8.8                                 | 3.16                      |
| TTTT                   | 1     | 1.71                                  | 0.03  | 7.2  | 1.07                                  | 0.70                                   | 0.38                                  | 4.5                                 | 2.25                      |
| GGGG'                  | 2     | 4.19                                  | 3.98  | 2.8  | 4.32                                  | 1.06                                   | 3.27                                  | 2.7                                 | 1.92                      |
| GG'G'G                 | 2     | 5.21                                  | 3.54  | 3.4  | 4.28                                  | 1.75                                   | 2.54                                  | 3.7                                 | 1.07                      |
| TTGG'                  | 2     | 3.97                                  | 2.03  | 6.3  | 2.98                                  | 2.53                                   | 0.45                                  | 8.7                                 | 3.18                      |
| TTTG                   | 2     | 3.41                                  | 1.52  | 7.8  | 2.63                                  | 2.63                                   | 0.00                                  | 10.5                                | 1.93                      |
| TGTT                   | 2     | 3.12                                  | 1.58  | 7.6  | 2.42                                  | 2.12                                   | 0.30                                  | 9.3                                 | 1.78                      |
| GTGG'                  | 2     | 5.07                                  | 3.30  | 3.7  | 4.17                                  | 2.17                                   | 2.01                                  | 4.6                                 | 1.57                      |
| TGTG                   | 2     | 4.37                                  | 2.78  | 4.6  | 3.63                                  | 2.15                                   | 1.47                                  | 5.7                                 | 1.97                      |
| TGGT                   | 2     | 3.47                                  | 3.01  | 4.2  | 3.37                                  | -0.61                                  | 3.98                                  | 2.0                                 | 1.31                      |
| GTTG                   | 2     | 5.35                                  | 3.42  | 3.5  | 4.56                                  | 0.98                                   | 3.58                                  | 2.4                                 | 1.62                      |
| GTG'G                  | 2     | 6.27                                  | 4.37  | 2.4  | 5.39                                  | 2.77                                   | 2.62                                  | 3.6                                 | 1.79                      |
| TTGG                   | 2     | 5.06                                  | 3.74  | 3.1  | 4.58                                  | 2.04                                   | 2.54                                  | 3.7                                 | 1.83                      |
| TGTG'                  | 2     | 5.58                                  | 3.84  | 3.0  | 4.75                                  | 2.40                                   | 2.35                                  | 4.0                                 | 2.26                      |
| GTTG'                  | 1     | 6.63                                  | 4.51  | 1.1  | 5.72                                  | 2.91                                   | 2.81                                  | 1.6                                 | 3.02                      |
| TGGG                   | 2     | 6.93                                  | 5.16  | 1.7  | 5.99                                  | 2.36                                   | 3.63                                  | 2.3                                 | 2.12                      |
| GTG'G'                 | 2     | 7.58                                  | 6.00  | 1.2  | 6.95                                  | 2.41                                   | 4.54                                  | 1.6                                 | 1.83                      |
| GGTG                   | 2     | 8.19                                  | 6.44  | 1.0  | 7.41                                  | 2.45                                   | 4.96                                  | 1.4                                 | 2.96                      |
| GGGG                   | 2     | 9.92                                  | 8.84  | 0.4  | 9.60                                  | 0.59                                   | 9.01                                  | 0.3                                 | 2.04                      |
| TGGT                   | 1     | 12.25                                 | 10.86   | 0.1  | 11.57                                 | 1.93                                   | 9.64                                  | 0.1                                 | 1.41                      |
| GGG'G'                 | 1     | 11.59                                 | 11.03   | 0.1  | 11.40                                 | 0.58                                   | 10.82                                 | 0.1                                 | 3.12                      |

<sup>a</sup> See Figure 1; <sup>b</sup>  $\Delta E_{zpvE}$ , zero-point vibrational energy corrected relative energies; <sup>c</sup> population according to  $\Delta E_{zpvE}$  values; <sup>d</sup> population according to  $\Delta G$  values; <sup>e</sup> 1 D =  $1/3 \times 10^{-2}$  C m

**Table S4** – Calculated (mPW1PW/6-31G\*) structural parameters for the most stable conformers of 1,3-dap in the different chemical environments considered.

| Parameter <sup>a</sup>                          | <i>Isolated molecule</i> |        | <i>Condensed phase</i> |       | <i>Aqueous Solution</i> |       | <i>CCl<sub>4</sub> solution</i> |        |
|---|--------------------------|--------|------------------------|-------|-------------------------|-------|---------------------------------|--------|
|   | GGG'G                    | TG'GG' | TTTG                   | TGTT  | TTTG                    | TGTT  | TTTG                            | TG'GG' |
| <i>Bond length (pm)</i>                         |                          |        |                        |       |                         |       |                                 |        |
| C <sup>4</sup> C <sup>7</sup>                   | 152.6                    | 153.5  | 152.3                  | 153.2 | 152.3                   | 153.2 | 152.3                           | 153.3  |
| C <sup>4</sup> H <sup>5</sup>                   | 110.4                    | 109.6  | 110.4                  | 109.8 | 110.4                   | 109.8 | 110.5                           | 109.7  |
| C <sup>4</sup> H <sup>6</sup>                   | 109.7                    | 109.8  | 109.7                  | 109.7 | 109.7                   | 109.7 | 109.7                           | 109.9  |
| C <sup>7</sup> C <sup>10</sup>                  | 152.6                    | 152.6  | 152.9                  | 152.9 | 152.9                   | 152.9 | 152.9                           | 152.7  |
| C <sup>7</sup> H <sup>8</sup>                   | 109.8                    | 110.0  | 109.8                  | 109.9 | 109.8                   | 109.9 | 109.7                           | 109.9  |
| C <sup>7</sup> H <sup>9</sup>                   | 109.7                    | 109.8  | 110.0                  | 110.0 | 110.0                   | 110.0 | 110.0                           | 109.8  |
| C <sup>10</sup> H <sup>11</sup>                 | 110.7                    | 109.7  | 109.7                  | 109.8 | 109.8                   | 109.8 | 109.7                           | 109.7  |
| C <sup>10</sup> H <sup>12</sup>                 | 109.7                    | 110.3  | 109.7                  | 109.7 | 109.8                   | 109.7 | 109.7                           | 110.3  |
| N <sup>1</sup> C <sup>4</sup>                   | 146.3                    | 145.6  | 146.2                  | 146.1 | 146.3                   | 146.2 | 146.0                           | 146.3  |
| N <sup>1</sup> H <sup>2</sup>                   | 101.6                    | 101.7  | 102.0                  | 101.9 | 102.1                   | 101.9 | 101.8                           | 102.1  |
| N <sup>1</sup> H <sup>3</sup>                   | 101.7                    | 101.9  | 102.1                  | 102.0 | 102.1                   | 102.1 | 101.8                           | 102.1  |
| N <sup>13</sup> C <sup>10</sup>                 | 145.7                    | 146.4  | 146.1                  | 146.1 | 146.2                   | 146.2 | 145.9                           | 146.6  |
| N <sup>13</sup> H <sup>14</sup>                 | 101.6                    | 101.7  | 102.1                  | 102.1 | 102.1                   | 102.1 | 101.8                           | 102.1  |
| N <sup>13</sup> H <sup>15</sup>                 | 101.8                    | 101.6  | 102.1                  | 102.1 | 102.1                   | 102.1 | 101.8                           | 102.0  |
| <i>Bond angle(°)</i>                            |                          |        |                        |       |                         |       |                                 |        |
| C <sup>4</sup> C <sup>7</sup> C <sup>10</sup>   | 114.8                    | 114.6  | 113.2                  | 114.3 | 113.2                   | 114.3 | 113.3                           | 114.5  |
| C <sup>4</sup> C <sup>7</sup> H <sup>8</sup>    | 109.9                    | 109.4  | 108.9                  | 108.9 | 108.9                   | 108.9 | 108.6                           | 109.3  |
| C <sup>4</sup> C <sup>7</sup> H <sup>9</sup>    | 107.6                    | 109.2  | 109.3                  | 109.2 | 109.3                   | 109.1 | 109.3                           | 109.1  |
| C <sup>7</sup> C <sup>10</sup> H <sup>11</sup>  | 108.3                    | 108.7  | 109.3                  | 109.2 | 109.3                   | 109.2 | 109.4                           | 108.7  |
| C <sup>7</sup> C <sup>10</sup> H <sup>12</sup>  | 108.5                    | 109.1  | 109.5                  | 109.8 | 109.5                   | 109.8 | 109.6                           | 108.9  |
| C <sup>7</sup> C <sup>10</sup> N <sup>13</sup>  | 111.1                    | 112.0  | 115.8                  | 115.8 | 115.7                   | 115.7 | 116.0                           | 112.2  |
| C <sup>10</sup> N <sup>13</sup> H <sup>14</sup> | 109.7                    | 109.4  | 108.7                  | 108.7 | 108.6                   | 108.6 | 109.1                           | 108.9  |
| C <sup>10</sup> N <sup>13</sup> H <sup>15</sup> | 107.7                    | 109.9  | 108.8                  | 108.8 | 108.6                   | 108.6 | 109.2                           | 109.2  |
| H <sup>2</sup> N <sup>1</sup> C <sup>4</sup>    | 110.0                    | 109.0  | 109.0                  | 109.9 | 108.9                   | 109.8 | 109.5                           | 108.1  |
| H <sup>2</sup> N <sup>1</sup> H <sup>3</sup>    | 106.5                    | 105.8  | 105.2                  | 105.6 | 105.0                   | 105.5 | 105.6                           | 104.9  |
| H <sup>3</sup> N <sup>1</sup> C <sup>4</sup>    | 109.5                    | 107.3  | 108.7                  | 109.2 | 108.5                   | 109.0 | 109.1                           | 106.0  |
| H <sup>5</sup> C <sup>4</sup> C <sup>7</sup>    | 108.7                    | 109.0  | 108.9                  | 109.4 | 108.9                   | 109.4 | 109.0                           | 109.2  |
| H <sup>5</sup> C <sup>4</sup> H <sup>6</sup>    | 106.5                    | 105.9  | 106.3                  | 106.1 | 106.3                   | 106.1 | 106.3                           | 106.1  |
| H <sup>6</sup> C <sup>4</sup> C <sup>7</sup>    | 108.9                    | 108.5  | 109.1                  | 108.8 | 109.1                   | 108.8 | 109.0                           | 108.5  |
| H <sup>8</sup> C <sup>7</sup> C <sup>10</sup>   | 108.3                    | 109.6  | 109.7                  | 108.7 | 109.6                   | 108.7 | 109.9                           | 109.6  |
| H <sup>8</sup> C <sup>7</sup> H <sup>9</sup>    | 106.8                    | 106.0  | 106.6                  | 106.4 | 106.6                   | 106.4 | 106.5                           | 106.2  |
| H <sup>9</sup> C <sup>7</sup> C <sup>10</sup>   | 109.2                    | 107.7  | 109.0                  | 109.1 | 109.0                   | 109.1 | 109.0                           | 107.8  |
| H <sup>11</sup> C <sup>10</sup> H <sup>12</sup> | 106.3                    | 106.4  | 106.1                  | 106.2 | 106.1                   | 106.2 | 106.0                           | 106.4  |
| H <sup>11</sup> C <sup>10</sup> N <sup>13</sup> | 114.2                    | 107.3  | 107.8                  | 107.9 | 107.9                   | 108.0 | 107.7                           | 107.5  |
| H <sup>12</sup> C <sup>10</sup> N <sup>13</sup> | 108.0                    | 113.2  | 107.8                  | 107.6 | 107.9                   | 107.6 | 107.7                           | 112.9  |
| H <sup>14</sup> N <sup>13</sup> H <sup>15</sup> | 107.6                    | 106.1  | 105.1                  | 105.0 | 104.9                   | 104.9 | 105.4                           | 105.5  |
| N <sup>1</sup> C <sup>4</sup> C <sup>7</sup>    | 111.9                    | 117.0  | 110.9                  | 116.8 | 111.0                   | 116.7 | 110.8                           | 116.3  |
| N <sup>1</sup> C <sup>4</sup> H <sup>5</sup>    | 113.3                    | 108.1  | 113.6                  | 107.6 | 113.5                   | 107.7 | 113.8                           | 108.1  |
| N <sup>1</sup> C <sup>4</sup> H <sup>6</sup>    | 107.3                    | 107.8  | 107.8                  | 107.6 | 107.9                   | 107.7 | 107.7                           | 108.0  |



*Dihedral angle(°)*

|   |        |        |        |        |        |        |         |        |
|---|--------|--------|--------|--------|--------|--------|---------|--------|
| C <sup>4</sup> C <sup>7</sup> C <sup>10</sup> H <sup>11</sup>   | -51.9  | -54.9  | 58.0   | 57.5   | 58.1   | 57.6   | 58.0    | -56.1  |
| C <sup>4</sup> C <sup>7</sup> C <sup>10</sup> H <sup>12</sup>   | -166.9 | -170.6 | -57.8  | -58.5  | -57.8  | -58.4  | -57.8   | -171.6 |
| C <sup>4</sup> C <sup>7</sup> C <sup>10</sup> N <sup>13</sup>   | 74.4   | 63.4   | -180.0 | 179.5  | -179.9 | 179.6  | 180.0   | 62.6   |
| C <sup>7</sup> C <sup>10</sup> N <sup>13</sup> H <sup>14</sup>  | -178.9 | 68.3   | -56.8  | -55.8  | -56.6  | -55.5  | -57.3   | 68.2   |
| C <sup>7</sup> C <sup>10</sup> N <sup>13</sup> H <sup>15</sup>  | -62.0  | -175.6 | 57.0   | 58.0   | 56.9   | 58.0   | 57.5    | -177.0 |
| H <sup>2</sup> N <sup>1</sup> C <sup>4</sup> C <sup>7</sup>     | 179.7  | -65.0  | 179.5  | -62.5  | 179.9  | -62.6  | 178.5   | -64.7  |
| H <sup>2</sup> N <sup>1</sup> C <sup>4</sup> H <sup>5</sup>     | -57.0  | 58.4   | -57.4  | 60.8   | -57.0  | 60.8   | -58.3   | 58.6   |
| H <sup>2</sup> N <sup>1</sup> C <sup>4</sup> H <sup>6</sup>     | 60.2   | 172.5  | 60.1   | 174.8  | 60.4   | 174.8  | 59.3    | 173.0  |
| H <sup>3</sup> N <sup>1</sup> C <sup>4</sup> C <sup>7</sup>     | -63.6  | 49.1   | -66.3  | 52.9   | -66.2  | 52.5   | -66.4   | 47.3   |
| H <sup>3</sup> N <sup>1</sup> C <sup>4</sup> H <sup>5</sup>     | 59.7   | 172.6  | 56.8   | 176.2  | 56.8   | 175.9  | 56.9    | 170.6  |
| H <sup>3</sup> N <sup>1</sup> C <sup>4</sup> H <sup>6</sup>     | 177.0  | -73.4  | 174.3  | -69.8  | 174.3  | -70.1  | 174.5   | -75.0  |
| H <sup>5</sup> C <sup>4</sup> C <sup>7</sup> C <sup>10</sup>    | 173.5  | 167.5  | 56.1   | -57.8  | 56.1   | -57.6  | 56.2    | 167.3  |
| H <sup>5</sup> C <sup>4</sup> C <sup>7</sup> H <sup>8</sup>     | -64.1  | -69.0  | 178.4  | 63.9   | 178.4  | 64.1   | 178.7   | -69.3  |
| H <sup>5</sup> C <sup>4</sup> C <sup>7</sup> H <sup>9</sup>     | 51.7   | 46.6   | -65.5  | 179.7  | -65.5  | 179.9  | -65.5   | 46.4   |
| H <sup>6</sup> C <sup>4</sup> C <sup>7</sup> C <sup>10</sup>    | 57.9   | 52.6   | -59.5  | -173.3 | -59.5  | -173.1 | -59.4   | 52.1   |
| H <sup>6</sup> C <sup>4</sup> C <sup>7</sup> H <sup>8</sup>     | -179.7 | 176.1  | 62.8   | -51.5  | 62.7   | -51.4  | 63.0    | 175.5  |
| H <sup>6</sup> C <sup>4</sup> C <sup>7</sup> H <sup>9</sup>     | -63.8  | -68.3  | 178.8  | 64.2   | 178.8  | 64.4   | 178.9   | -68.8  |
| H <sup>8</sup> C <sup>7</sup> C <sup>10</sup> H <sup>11</sup>   | -175.1 | -178.3 | -63.8  | -64.3  | -63.8  | -64.2  | -63.7   | -179.3 |
| H <sup>8</sup> C <sup>7</sup> C <sup>10</sup> H <sup>12</sup>   | 69.9   | 66.0   | -179.7 | 179.7  | -179.7 | 179.8  | -179.6  | 65.2   |
| H <sup>8</sup> C <sup>7</sup> C <sup>10</sup> N <sup>13</sup>   | -48.8  | -60.0  | 58.2   | 57.7   | 58.2   | 57.8   | 58.2    | -60.6  |
| H <sup>9</sup> C <sup>7</sup> C <sup>10</sup> H <sup>11</sup>   | 69.0   | 66.8   | 179.9  | -180.0 | 179.9  | -179.9 | 179.9   | 65.5   |
| H <sup>9</sup> C <sup>7</sup> C <sup>10</sup> H <sup>12</sup>   | -46.0  | -48.8  | 64.0   | 64.0   | 64.1   | 64.1   | 64.1    | -50.0  |
| H <sup>9</sup> C <sup>7</sup> C <sup>10</sup> N <sup>13</sup>   | -164.7 | -174.9 | -58.1  | -58.0  | -58.1  | -57.9  | -58.1   | -175.7 |
| H <sup>11</sup> C <sup>10</sup> N <sup>13</sup> H <sup>14</sup> | -55.9  | -172.6 | 66.0   | 66.9   | 66.1   | 67.1   | 65.5    | -172.3 |
| H <sup>11</sup> C <sup>10</sup> N <sup>13</sup> H <sup>15</sup> | 61.0   | -56.4  | 179.8  | -179.3 | 179.7  | -179.4 | -179.7  | -57.6  |
| H <sup>12</sup> C <sup>10</sup> N <sup>13</sup> H <sup>14</sup> | 62.2   | -55.5  | -179.9 | -178.9 | -179.6 | -178.6 | 179.5   | -55.3  |
| H <sup>12</sup> C <sup>10</sup> N <sup>13</sup> H <sup>15</sup> | 179.0  | 60.7   | -66.0  | -65.1  | -66.0  | -65.1  | -65.7   | 59.5   |
| N <sup>1</sup> C <sup>4</sup> C <sup>7</sup> H <sup>8</sup>     | 61.7   | 54.0   | -55.8  | -173.6 | -56.0  | -173.4 | -55.3   | 53.5   |
| N <sup>1</sup> C <sup>4</sup> C <sup>7</sup> H <sup>9</sup>     | 177.6  | 169.6  | 60.2   | -57.8  | 60.1   | -57.6  | 60.5    | 169.2  |
| N <sup>1</sup> C <sup>4</sup> C <sup>7</sup> C <sup>10</sup>    | -60.6  | -69.5  | -178.2 | 64.7   | -178.3 | 64.9   | -177.83 | -69.9  |

<sup>a</sup> See Figure 1 for atom numbering